VEGF-A regulates cellular localization of SR-BI as well as transendothelial transport of HDL but not LDL

Velagapudi, Srividya ; Yalcinkaya, Mustafa ; Piemontese, Antonio ; Meier, Roger ; Nørrelykke, Simon Flyvbjerg ; Perisa, Damir ; Rzepiela, Andrzej ; Stebler, Michael ; Stoma, Szymon ; Zanoni, Paolo ; Rohrer, Lucia ; von Eckardstein, Arnold

Abstract: OBJECTIVE: Low- and high-density lipoproteins (LDL and HDL) must pass the endothelial layer to exert pro- and antiatherogenic activities, respectively, within the vascular wall. However, the rate-limiting factors that mediate transendothelial transport of lipoproteins are yet little known. Therefore, we performed a high-throughput screen with kinase drug inhibitors to identify modulators of transendothelial LDL and HDL transport. APPROACH AND RESULTS: Microscopy-based high-content screening was performed by incubating human aortic endothelial cells with 141 kinase-inhibiting drugs and fluorescent-labeled LDL or HDL. Inhibitors of vascular endothelial growth factor (VEGF) receptors (VEGFR) significantly decreased the uptake of HDL but not LDL. Silencing of VEGF receptor 2 significantly decreased cellular binding, association, and transendothelial transport of (125)I-HDL but not (125)I-LDL. RNA interference with VEGF receptor 1 or VEGF receptor 3 had no effect. Binding, uptake, and transport of HDL but not LDL were strongly reduced in the absence of VEGF-A from the cell culture medium and were restored by the addition of VEGF-A. The restoring effect of VEGF-A on endothelial binding, uptake, and transport of HDL was abrogated by pharmacological inhibition of phosphatidyl-inositol 3 kinase/protein kinase B or p38 mitogen-activated protein kinase, as well as silencing of scavenger receptor BI. Moreover, the presence of VEGF-A was found to be a prerequisite for the localization of scavenger receptor BI in the plasma membrane of endothelial cells. CONCLUSIONS: The identification of VEGF as a regulatory factor of transendothelial transport of HDL but not LDL supports the concept that the endothelium is a specific and, hence, druggable barrier for the entry of lipoproteins into the vascular wall.

DOI: https://doi.org/10.1161/ATVBAHA.117.309284

VEGF-A Regulates Cellular Localization of SR-BI as Well as Transendothelial Transport of HDL but Not LDL

Srividya Velagapudi, Mustafa Yalcinkaya, Antonio Piemontese, Roger Meier, Simon Flyvbjerg Nørrelykke, Damir Perisa, Andrzej Rzepiela, Michael Stebler, Szymon Stoma, Paolo Zanoni, Lucia Rohrer,* Arnold von Eckardstein*

Objective—Low- and high-density lipoproteins (LDL and HDL) must pass the endothelial layer to exert pro- and antiatherogenic activities, respectively, within the vascular wall. However, the rate-limiting factors that mediate transendothelial transport of lipoproteins are yet little known. Therefore, we performed a high-throughput screen with kinase drug inhibitors to identify modulators of transendothelial LDL and HDL transport.

Approach and Results—Microscopy-based high-content screening was performed by incubating human aortic endothelial cells with 141 kinase-inhibiting drugs and fluorescent-labeled LDL or HDL. Inhibitors of vascular endothelial growth factor (VEGF) receptors (VEGFR) significantly decreased the uptake of HDL but not LDL. Silencing of VEGF receptor 2 significantly decreased cellular binding, association, and transendothelial transport of ^{125}I-HDL but not ^{125}I-LDL. RNA interference with VEGF receptor 1 or VEGF receptor 3 had no effect. Binding, uptake, and transport of HDL but not LDL were strongly reduced in the absence of VEGF-A from the cell culture medium and were restored by the addition of VEGF-A. The restoring effect of VEGF-A on endothelial binding, uptake, and transport of HDL was abrogated by pharmacological inhibition of phosphatidyl-inositol 3 kinase/protein kinase B or p38 mitogen-activated protein kinase, as well as silencing of scavenger receptor BI. Moreover, the presence of VEGF-A was found to be a prerequisite for the localization of scavenger receptor BI in the plasma membrane of endothelial cells.

Conclusions—The identification of VEGF as a regulatory factor of transendothelial transport of HDL but not LDL supports the concept that the endothelium is a specific and, hence, druggable barrier for the entry of lipoproteins into the vascular wall.

Visual Overview—An online visual overview is available for this article. **(*Arterioscler Thromb Vasc Biol*. 2017;37:794-803. DOI: 10.1161/ATVBAHA.117.309284.)**

Key Words: atherosclerosis ■ endothelial cells ■ HDL ■ SR-BI ■ VEGF-A

Accumulation of low-density lipoproteins (LDL) and lipids in the subendothelial matrix and macrophages is crucial in the pathogenesis of atherosclerosis.[1] Conversely, removal of cholesterol from the subendothelial space by cholesterol efflux and subsequent reverse cholesterol transport have been postulated to confer protection against atherosclerosis.[2] To reach the subendothelial space, both LDL and high-density lipoprotein (HDL) have to cross the intact endothelial barrier. It is yet controversial whether transendothelial HDL transport is mediated by specific mechanisms or the result of passive filtration.[3,4] Our laboratory previously showed that aortic endothelial cells are able to specifically bind, internalize, and transport HDL in a saturable and temperature-dependent manner via a nonclassical endocytic route involving dynamin and cytosketal networks.[5,6] We also demonstrated that transcytosis of mature HDL is regulated by ATP-binding cassette transporter ABCG1, scavenger receptor BI (SR-BI), and endothelial lipase, as well as the ectopic-β ATPase/purinergic receptor axis.[6–8] Other laboratories reported that endothelial cells internalize LDL by at least 2 pathways[3]: The classical one leads to lysosomal degradation and involves clathrin-coated pits and the LDL receptor.[9,10] The other nondegrading pathway allows the transendothelial transport of LDL and involves caveolae,[11] SR-BI,[12] and activin-like kinase 1.[13]

Genome-wide RNA interference studies have shown that both clathrin- and caveolin-dependent endocytosis are regulated by kinases.[14] The kinases regulating the endocytosis of lipoproteins especially by endothelial cells are unknown. To identify such signaling cascades regulating the uptake of LDL and HDL, we performed a microscopy-based high-content screening on human aortic endothelial cells (HAECs) using a kinase inhibitor drug library. Starting with

Received on: November 28, 2016; final version accepted on: March 20, 2017.

From the Institute of Clinical Chemistry, University and University Hospital of Zurich, Schlieren, Switzerland (S.V., M.Y., A.P., D.P., P.Z., L.R., A.v.E.); Competence Center for Integrated Human Physiology, University of Zurich, Switzerland (S.V., M.Y., D.P., P.Z., L.R., A.v.E.); Department of Pharmacy, University of Parma, Italy (A.P.); and Scientific Center for Optical and Electron Microscopy, ETH Zurich, Switzerland (R.M., S.F.N., A.R., M.S., S.S.).

*These authors contributed equally to this article.

The online-only Data Supplement is available with this article at http://atvb.ahajournals.org/lookup/suppl/doi:10.1161/ATVBAHA.117.309284/-/DC1.

Correspondence to Arnold von Eckardstein, MD, Institute of Clinical Chemistry, University Hospital Zurich, Rämistrasse 100, Zurich, 8951, Switzerland. E-mail arnold.voneckardstein@usz.ch; or Lucia Rohrer, PhD, Institute of Clinical Chemistry, University Hospital Zurich, Wagistrasse 14, Schlieren, 8952, Switzerland. E-mail lucia.rohrer@usz.ch

Nonstandard Abbreviations and Acronyms	
Akt	protein kinase B
HAEC	human aortic endothelial cells
HDL	high-density lipoprotein
LDL	low-density lipoprotein
MEK	mitogen-activated protein kinase kinase
p38 MAPK	p38 mitogen-activated protein kinase
PI3K	phosphatidylinositol-4,5-bisphosphate 3-kinase
SR-BI	scavenger receptor class B type I
VEGF	vascular endothelial growth factor
VEGFR	vascular endothelial growth factor receptor

this unbiased strategy, we found evidence for an important regulatory role of vascular endothelial growth factor (VEGF) and its cognate VEGF receptor-2 (VEGFR2), as well as its downstream signaling kinases in regulating uptake of HDL but not LDL by endothelial cells. The validation of this discovery did not only confirm the findings of the screen but also unraveled a regulatory role of VEGF-A on the subcellular trafficking of SR-BI.

Materials and Methods

Materials and Methods are available in the online-only Data Supplement.

Results

Screening of Kinase Inhibitors

After culture for 72 hours in 384 well plates at a density of 1000 cells per well, HAECs were treated with 141 kinase-inhibiting drugs for 1 hour at 7 different dilutions spanning 4 orders of magnitude. Thereafter, cells were incubated with fluorescent-labeled Atto 594-LDL or Atto 594-HDL for another hour. After washing, fixation, and nuclei staining, 9 images per well were acquired using a molecular devices wide-field microscope. The microscope-generated images were processed by Cell profiler to segment nuclei and RFP (red fluorescent protein) foci intensity (vesicles) per cell. For each compound interaction, the amount of downregulation was calculated relative to a control reaction in the presence of vehicle (dimethyl sulfoxide). The analysis of the dose-response data for LDL and HDL uptake by the use of the Hill model (see methods) identified 2 and 9 drugs, respectively, with a Hill coefficient of 4, which, therefore, were suspicious of toxicity and, hence, excluded from further analysis (Tables I and II in the online-only Data Supplement). The drugs were preclassified as active based on their ability to fit the Hill logistic model only when the RFP foci signal dropped >50%. Finally, using Fisher exact test, we statistically evaluated the probability of finding drugs targeting a kinase that actively decrease the uptake of fluorescent LDL or HDL in the presence of maximal concentration versus nontargeting drugs. After correction of *P* values for multiple statistical testing, VEGFR emerged as the only target whose inhibition significantly interfered with the HDL uptake by HAECs. However, this analysis did not reveal any target whose inhibition led to a significant and consistent decrease in LDL uptake (Table).

VEGFR2 Regulates Endothelial Binding, Association, and Transport of HDL but Not LDL

We first confirmed the regulatory role of VEGFR in the uptake of HDL by HAECs and to identify the relevant VEGF receptor by a knockdown strategy. HAECs expressed all 3 VEGF receptors: VEGFR1, VEGFR2, and VEGFR3 as analyzed by quantitative reverse transcriptase polymerase chain reaction (Figure IA in the online-only Data Supplement). To test which VEGF receptor was involved in HDL uptake, each of the 3 VEGF receptors was targeted using RNA interference. Although knockdown was efficient for each VEGFR on the mRNA level (Figure IB in the online-only Data Supplement) and protein level (Figure IC in the online-only Data Supplement), only the silencing of VEGFR2 decreased the cellular uptake of fluorescent-labeled Atto594-HDL, whereas silencing VEGFR1 and VEGFR3 showed no effect (left lane of Figure II in the online-only Data Supplement). These findings were confirmed using radioiodinated HDL, where silencing of VEGFR2 significantly reduced the specific 4°C binding of ^{125}I-HDL to endothelial cells by 60% (Figure 1A), the specific 37°C cellular association by 80% (Figure 1B), and the specific transendothelial transport of ^{125}I-HDL from apical to basal compartment at 37°C by 60% (Figure 1C). However, neither cellular uptake of fluorescent-labeled Atto488-LDL (right lane of Figure II in the online-only Data Supplement) nor specific cellular binding, association, and transendothelial transport of ^{125}I-LDL were affected by silencing of any VEGF receptor (Figure 1D through 1F). Taken together, these results indicate a specific effect of VEGFR2 on endothelial binding and uptake, as well as transendothelial transport of HDL but not LDL.

VEGF-A Regulates Endothelial Binding, Association, and Transport of HDL but Not LDL

Binding of VEGF-A to its receptor VEGFR2 induces conformational changes and receptor dimerization, which in turn triggers kinase activation and autophosphorylation of tyrosine residues.[15] To investigate whether VEGF-A regulates transendothelial transport of HDL, we cultured endothelial cells either in the VEGF-A-containing medium A or in the VEGF-A-free medium B. The presence or absence of VEGF in the medium had no effect on the proliferation of HAECs (Figure IIIA in the online-only Data Supplement). On Western blot analysis, we found that HAECs cultured in VEGF-free medium for 72 hours lose phosphorylation of Tyr residues 1054 and 1059 in the major tyrosine kinase catalytic domain of VEGFR2 (Figure IIIB in the online-only Data Supplement).

As shown in the left panel of Figure IV in the online-only Data Supplement, cells cultured in VEGF-free medium for 72 hours decreased the cellular uptake of Atto594-HDL compared with cells cultured in VEGF-containing medium (control). Interestingly, pretreatment of cells cultured in medium B supplemented with 25 ng/mL VEGF-A for 1 hour showed a significant increase in the uptake of Atto594-HDL (lowest figure in the left lane). Confirming these microscopic findings, pretreatment of cells for 1 hour with VEGF-A significantly increased 4°C cellular binding of ^{125}I-HDL (Figure 2A) and 37°C cellular association of ^{125}I-HDL (Figure 2B), as well as apical to basolateral transendothelial

Table. Fisher Exact Test Analysis of Binary Activity Signal for Uptake of LDL and HDL

	LDL					HDL				
Target	n	m	n′	m′	*P* Value	n	m	n′	m′	*P* Value
ABL	1	5	26	113	0.71653	2	4	51	88	0.714
ALK	1	3	26	115	0.56562	1	3	52	89	0.842
c-Kit	1	6	26	112	0.77159	3	4	50	88	0.505
c-Met	4	7	23	111	0.12361	5	6	48	86	0.369
EGFR	3	11	24	107	0.50494	8	6	45	86	0.084
FGFR	2	4	25	114	0.31014	3	3	50	89	0.383
FLT-3	0	1	27	117	1	0	1	53	91	1
HER2	2	5	25	113	0.38616	4	3	49	89	0.221
IGF-1R	1	0	26	118	0.18621	1	0	52	92	0.366
VEGFR	9	22	18	96	0.08137	18	13	35	79	0.005*
Aurora	5	10	22	108	0.11871	7	8	46	84	0.278
CDK	2	6	25	112	0.45878	1	7	52	85	0.977
CHK	0	1	27	117	1	0	1	53	91	1
GSK-3	0	3	27	115	1	0	3	53	89	1
JNK	0	1	27	117	1	0	1	53	91	1
JAK/STAT	1	3	26	115	0.56562	0	4	53	88	1
MEK	1	10	26	108	0.90542	4	7	49	85	0.623
mTOR	0	10	27	108	1	1	9	52	83	0.991
PI3K/AKT	1	17	26	101	0.98121	2	16	51	76	0.998
p38 MAPK	2	5	25	113	0.38616	2	5	51	87	0.798

For each target, Fisher exact test analysis was used to calculate the probability to get more active drugs (m) and less active drugs (n) for a given target and at the same time less active drugs (m′) and more active (n′) drugs for nontargets. The drugs were preclassified as active based on their ability to fit the Hill logistic model only when the RFP (red fluorescent protein) foci signal dropped >50%. ABL indicates Abelson murine leukemia viral oncogene homolog 1; AKT, protein kinase B; ALK, anaplastic lymphoma kinase; Aurora, Aurora kinase; c-Kit, tyrosine-protein kinase kit or CD117; c-Met, tyrosine-protein kinase met; CDK, cyclin-dependent kinase; CHK, check-point kinase; EGFR, epidermal growth factor receptor; FGFR, fibroblast growth factor receptor; FLT-3, fms-like tyrosine kinase 3; GSK-3, glycogen synthase kinase-3; HDL, high-density lipoprotein; HER2, receptor tyrosine-protein kinase erbB-2 or CD340; IGF-1R, insulin growth factor receptor; JAK/STAT, Janus kinase and signal transducer and activator of transcription proteins; JNK, c-Jun N-terminal kinase; LDL, low-density lipoprotein; MEK, mitogen-activated protein kinase kinase; mTOR, mammalian target of rapamycin; p38 MAPK, p38 mitogen-activated protein kinase; PI3K/AKT, phosphotidyl-inositol 3 kinase/protein kinase B; and VEGFR, vascular endothelial growth factor receptor.

Inhibition of targets with *$P \leq 0.01$ are interpreted to be more likely than the inhibition of all other targets to decrease the uptake of LDL or HDL. The data were obtained from 2 replicate experiments.

transport of ^{125}I-HDL (Figure 2C) compared with cells cultured in VEGF-free medium.

By contrast, cells cultured in VEGF-free medium for 72 hours did not show any decrease in the uptake of Atto488-LDL compared with the control condition (right lane of Figure IV in the online-only Data Supplement). Likewise, presence, absence, or supplementation of VEGF-A had no effect on the cellular binding, association, and transport of ^{125}I-LDL (Figure 2D, 2E, and 2F).

Taken together, these results indicate that VEGF-mediated VEGFR2 receptor activation is required for endothelial binding and uptake, as well as transendothelial transport of HDL but not LDL.

VEGF-A Regulates Endothelial Binding and Association of HDL Through p38 Mitogen-Activated Protein Kinase and Phosphatidyl-inositol 3 Kinase/Protein Kinase B

We determined whether the pharmacological inhibition of the downstream kinases of VEGF signaling, namely phosphatidyl-inositol 3 kinase (PI3K), p38 mitogen activated protein kinase (p38 MAPK), and mitogen-activated protein kinase kinase (MEK), interfere with endothelial binding and association of HDL. Cells were pretreated with indicated drugs for 30 minutes followed by pretreatment with 25 ng/mL of VEGF-A for 1 hour at 37°C. Western blot analysis revealed that residue Ser473 of protein kinase B (Akt; the downstream kinase targeted by PI3K), residues Thr180 and Tyr182 of p38 MAPK, and residues Thr202, Tyr204, Thr185, and Tyr187 of p44/42 MAPK (ERK1/2 [extracellular signal-regulated kinase], which is a common kinase target of MEK1 and MEK2) were phosphorylated in the presence but not in the absence of VEGF (Figure IIIB in the online-only Data Supplement). Treatment with either the PI3K inhibitor wortmannin or the Akt inhibitor MK 2206 or the p38 MAPK inhibitor PD169316 decreased the cellular binding and association of ^{125}I-HDL. These inhibitory effects were not overcome by pretreatment with VEGF-A. Also the dual MEK1 and MEK2 inhibitor U0126 significantly decreased the cellular binding and association of ^{125}I-HDL. However, by contrast

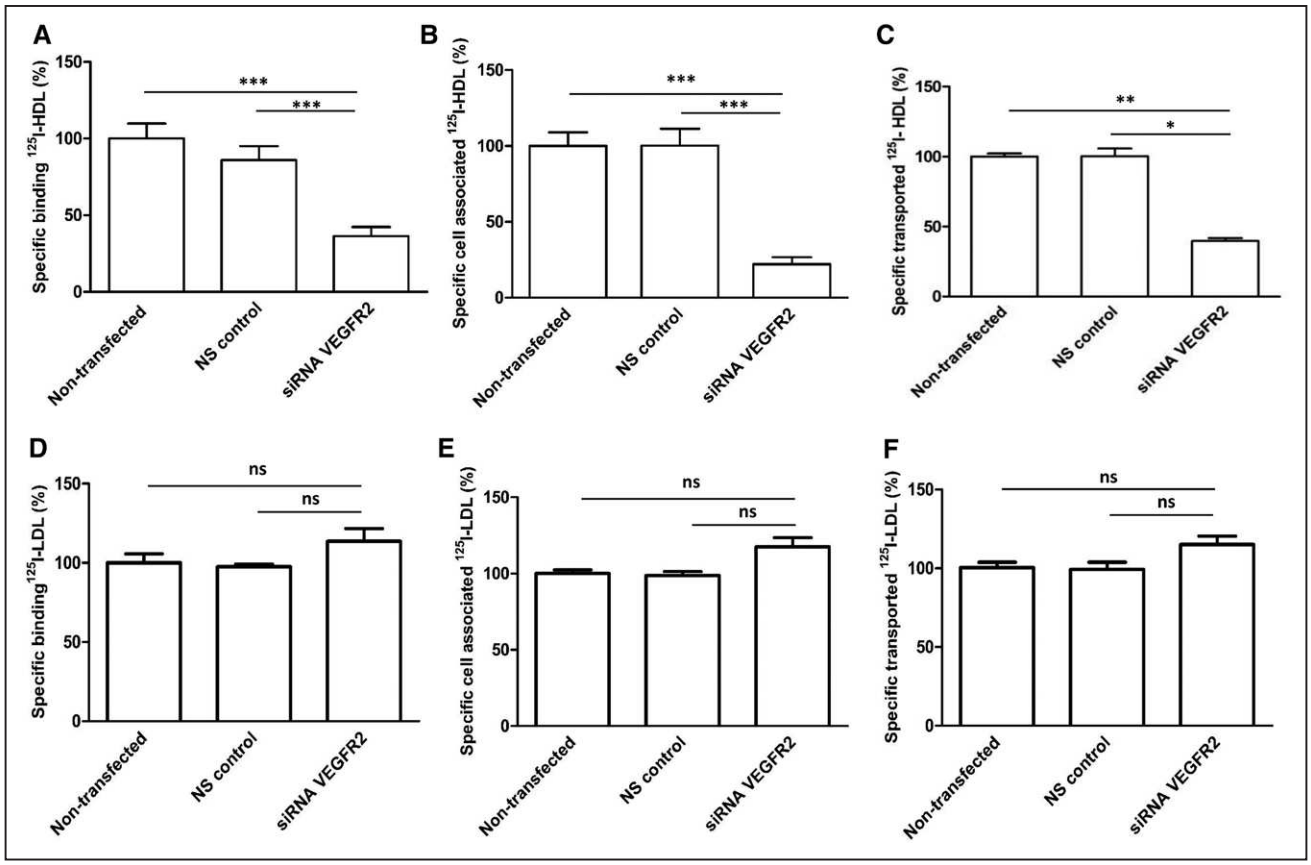

Figure 1. Vascular endothelial growth factor receptor 2 (VEGFR2) mediates binding, association, and transendothelial transport of high-density lipoprotein (HDL) but not low-density lipoprotein (LDL) in human aortic endothelial cells (HAECs). HAECs were transfected with a specific siRNA against VEGFR2 or with nonsilencing control siRNA (NS control), and assays were performed 72 hours after transfection. To study cellular binding, association, and transport, transfected endothelial cells (ECs) were incubated with 10 μg/mL of ^{125}I-HDL or ^{125}I-LDL for 1 hour in the absence (total) or in the presence of 40-fold excess of unlabeled HDL and LDL, respectively, to record unspecific interactions. Specific binding, association, and transport were calculated by subtracting unspecific values from total values. **A**, Specific binding was measured by incubating cells with ^{125}I-HDL (**A**) or ^{125}I-LDL (**D**) at 4°C. To measure specific cell association, cells were incubated with ^{125}I-HDL (**B**) or ^{125}I-LDL (**E**) at 37°C. For the measurement of transport, HAECs were cultured on inserts. The transport of ^{125}I-HDL (**C**) and ^{125}I-LDL (**F**) from the apical to basolateral compartment was measured at 37°C. The results are represented as means±SEM of 3 independent triplicate experiments (n=3). ***P≤0.001, **P≤0.01, *P≤0.05, and ns indicates not significant.

to wortmannin, MK 2206, and PD169316, pretreatment with VEGF-A restored the inhibitory effect of U0126 on endothelial binding and association of HDL (Figure 3A and 3B). The effects of pharmacological inhibitors were confirmed by using RNA interference of Akt, p38 MAPK, and MEK1/MEK2. The knockdown was found efficient for each kinase on the protein level (Figure V in the online-only Data Supplement). Like the pharmacological inhibitors, silencing of either Akt or p38 MAPK or MEK1/2 decreased the cellular binding and association of ^{125}I-HDL. Also on RNA interference, VEGF-A treatment restored the cellular binding and association of ^{125}I-HDL by endothelial cells lacking MEK1/2 but not by endothelial cells lacking Akt or p38 MAPK. (Figure VI in the online-only Data Supplement). Taken together, these results show that VEGF-induced binding and association of HDL depends on the activation of PI3K/Akt and p38 MAPK but is independent of the MEK/ERK pathway. Interestingly, endothelial binding or cell association of ^{125}I-LDL was not affected by silencing of Akt but significantly decreased by silencing of p38 MAPK and MEK (Figure VII in the online-only Data Supplement).

VEGF-A Regulates Binding, Association, and Transport of HDL via SR-BI

We have previously demonstrated that SR-BI, ABCG1, and endothelial lipase regulate binding and transendothelial transport of HDL. Because of the fast effects of VEGF-A on cellular binding, association, and transport of ^{125}I-HDL, we hypothesized that VEGF-A regulates the availability of one of these HDL interacting proteins on the cell surface in HAECs. To test this hypothesis, we performed a cell surface biotinylation experiment. HAECs cultured in the VEGF-free cell culture medium did not show any SR-BI on the cell surface. Pretreatment with VEGF-A restored the expression of cell surface SR-BI. By contrast, the presence or absence of VEGF-A had no effect on the cell surface expression of LDL receptor, ABCG1, or endothelial lipase (Figure 4). To determine whether VEGF-A regulated HDL transendothelial transport through SR-BI, we silenced SR-BI using RNA interference. The knockdown was efficient at the mRNA (Figure VIIIA in the online-only Data Supplement) and protein levels (Figure VIIIB in the online-only Data Supplement). Silencing SR-BI alone significantly decreased ^{125}I-HDL cellular binding

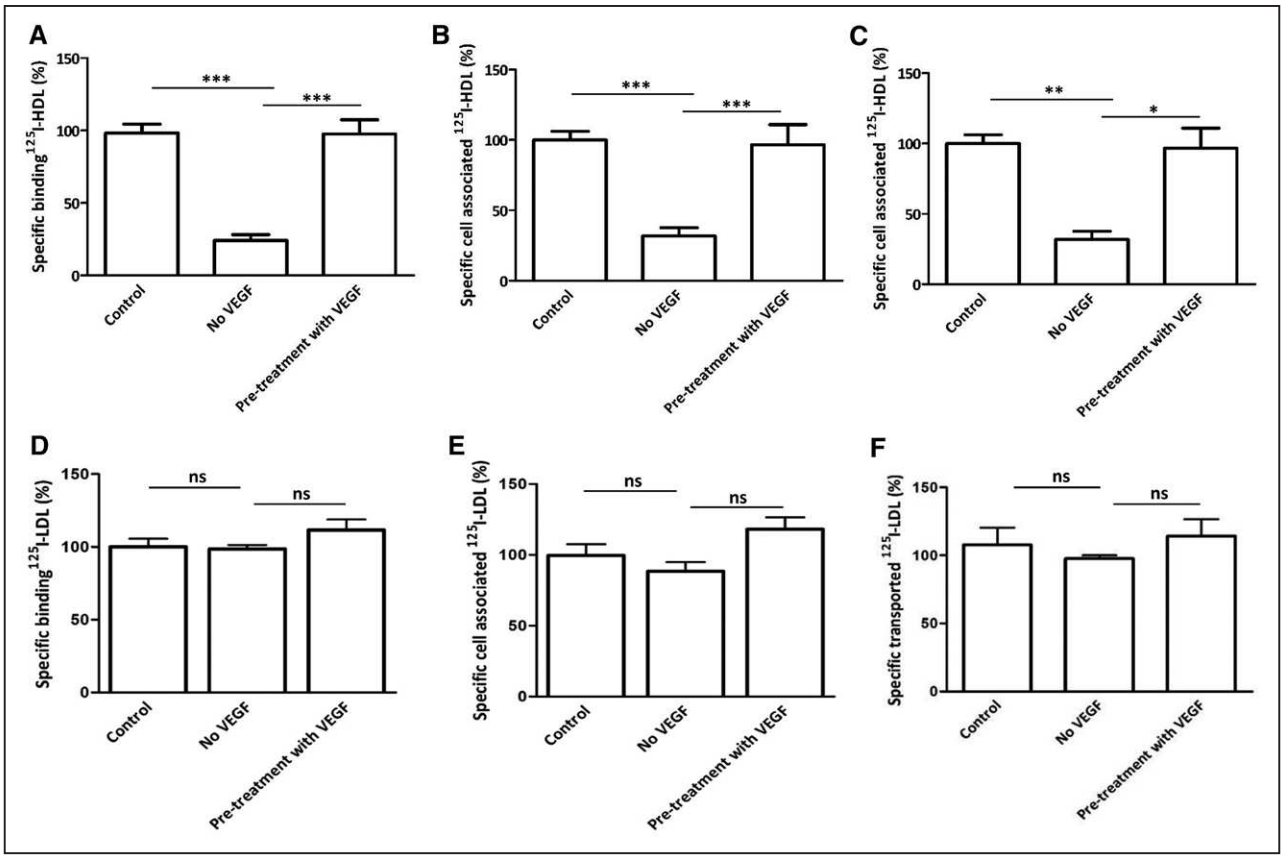

Figure 2. Effect of vascular endothelial growth factor (VEGF)-A on binding, association, and transendothelial transport of high-density lipoprotein (HDL) and low-density lipoprotein (LDL) in human aortic endothelial cells (HAECs). HAECs were cultured in medium containing VEGF-A (control) or lacking VEGF-A (no VEGF) for 72 hours. Cells were pretreated with 25 ng/mL of VEGF-A_{165} for 1 hour prior to the assays if indicated. Specific binding was measured by incubating cells with ^{125}I-HDL (**A**) and ^{125}I-LDL (**D**) at 4°C. Specific cell association was analyzed by incubating cells with ^{125}I-HDL (**B**) and ^{125}I-LDL (**E**) at 37°C. HAECs were cultured on inserts, and transport of ^{125}I-HDL (**C**) and ^{125}I-LDL (**F**) from the apical to basolateral compartment was measured at 37°C. The results are represented as mean±SEM of 3 independent triplicate experiments (n=3). ***P≤0.001, **P≤0.01, *P≤0.05, and ns indicates not significant.

and association by 50% to 55% and transport by 60%, respectively. Pretreatment with VEGF-A for 1 hour did not restore the cellular binding, association, and transport of ^{125}I-HDL inhibited by suppression of SR-BI (Figure 5A through 5C).

Discussion

We previously reported that bovine aortic endothelial cells bind, internalize, and transport HDL in a specific process dependent on SR-BI, ABCG1,[6] endothelial lipase,[7] and ectopic β-ATPase.[8] Here we show that HAECs also bind, internalize, and transport HDL, as well as LDL. Using a high-content drug screening approach, we identified VEGF-A/VEGFR2 signaling as a rate-limiting factor for the cell surface abundance of SR-BI and, as a consequence, regulator of uptake and transport of HDL by HAECs. Interestingly, VEGF-A and VEGFR2 had no effect on endothelial binding, uptake, and transport of LDL.

VEGFs are important regulators of both vasculogenesis and angiogenesis in the adult.[16] In mammals, the VEGF family encompasses 5 different isoforms namely, VEGF-A, -B, -C, and –D, as well as placenta growth factor. These ligands bind to 3 VEGF receptors—VEGFR1, VEGFR2, and VEGFR3—in an overlapping pattern. VEGF-A, VEGF-B, and placenta growth factor bind to VEGFR1[17–19]; VEGF-A binds to VEGFR2[20]; VEGF-C and VEGF-D bind to VEGFR3.[21,22] Among VEGF-A receptors, VEGFR1 has the highest affinity and acts as a negative regulator by sequestering VEGF-A from binding to VEGFR2[23]; hence, VEGFR2 is the key receptor mediating most of the cellular effects of VEGF-A in endothelial cells. In accordance with this, our results show that RNA interference with VEGFR2 but not with VEGFR1 decreases HDL uptake (Figure II in the online-only Data Supplement). Our data show some analogy with those reported by Lim et al[24] and Martel et al,[25] who observed improved lymphatic function and transport of HDL after VEGF-C treatment in mice.

Binding of VEGF-A induces conformational changes and dimerization of VEGFR2, which in turn triggers kinase activation, tyrosine phosphorylation of the dimerized VEGFR2, and subsequent phosphorylation of SH2-containing intracellular signaling proteins, including phospholipase C-γ1, Src family tyrosine kinases, and PI3K and Ras GTPase-activating protein residues of Ras-Raf-MEK-MAPK pathway.[26–29] VEGF was also shown to induce actin remodeling through activation of CDC42 and p38 MAPK.[30] Both by pharmacological inhibition and RNA interference, we revealed the involvement of PI3K/Akt, p38 MAPK, and the Ras-Raf-MEK pathway in binding and uptake of HDL (Figure 3;

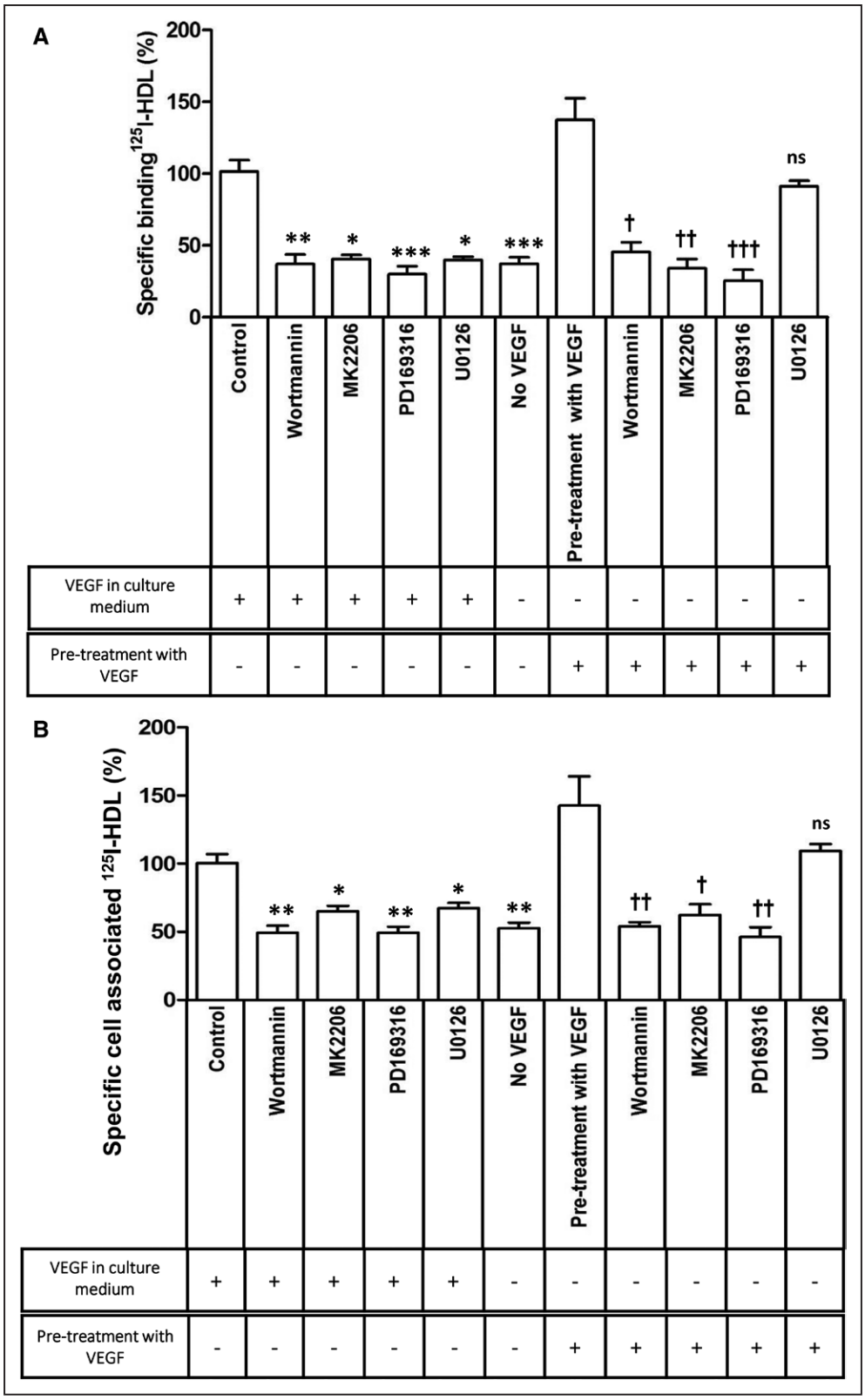

Figure 3. Vascular endothelial growth factor (VEGF)-A regulates high-density lipoprotein (HDL) binding and association through phosphatidyl-inositol 3 kinase/protein kinase B (PI3K/Akt) and p38 mitogen-activated protein kinase (p38 MAPK). Human aortic endothelial cells (HAECs) were cultured in the presence or absence of VEGF-A for 72 hours. Cells were then treated with Wortmannin (200 nM), or MK2206 (1 μM), or U0126 (10 μM), or PD169316 (100 nM) for 30 min, followed by treatment with 25 ng/mL VEGF-A_{165} for 1 hour at 37°C if indicated. **A**, Specific binding was measured by incubating cells with ^{125}I-HDL at 4°C. **B**, Specific cell association was analyzed by incubating cells with ^{125}I-HDL at 37°C. The results are represented as means±SEM of 3 independent triplicate experiments (n=3). ***$P \leq 0.001$, **$P \leq 0.01$, *$P \leq 0.05$. †††$P \leq 0.001$, ††$P \leq 0.01$, †$P \leq 0.05$, and ns indicates not significant.

Figure VI in the online-only Data Supplement). However, the inhibition of the Ras-Raf-MEK pathway but not the inhibition of PI3K/Akt and p38 MAPK could be overcome by VEGF stimulation. Thus, VEGF regulates the interaction of HDL with endothelial cells by activating PI3K/Akt and p38 MAPK but not the Ras-Raf-MEK pathway. PI3K is known to be involved in endosomal membrane trafficking,[31,32] and its inhibition by wortmannin in polarized cells affects early trafficking in the endocytic pathway, as well as inward vesicularization for the formation of multivesicular bodies in the later stages.[33] For example, PI3K was shown to mediate the stimulatory effect of insulin on the cell surface translocation of the glucose transporter-4.[32,34] It has also been shown in hepatocytes that insulin regulates the cell surface expression of SR-BI and selective lipid uptake dependent on PI3K activation.[35] VEGF-A is known to stimulate actin reorganization, which in turn contributes to HDL uptake[5] and cell migration depending on activation of p38 MAPK but not ERK1/2 MAP kinase.[36,37] Thus, it will be interesting to identify agonists beyond VEGF that regulate the endothelial binding, uptake, and transport of HDL by activating the MEK pathway. In this regard, it is also important to note our finding that RNA interference with MEK but not with Akt inhibited the binding and association of LDL with endothelial cells (Figure VII in the online-only Data Supplement).

We found that in HAECs, VEGF-A is required for the translocation of SR-BI from intracellular compartments to the cell surface, which in turn facilitates the binding, uptake, and transport of HDL (Figures 4 and 5). Similarly the cell-surface translocation of SR-BI is enhanced by insulin in hepatocytes[35] and by both insulin and angiotensin-II in adipocytes.[38]In hepatocytes, cell surface expression of SR-BI was shown to be dependent on PDZK1,[39] which is a tissue-specific adaptor protein with 4 PDZ domains (named after 3 proteins containing such domains: postsynaptic density protein [PSD95], Drosophila discs large [Dlg], and the tight junction protein zonula occludens-1 [ZO-1]). However, in our hands, interference with PDZK1 did not limit the binding of HDL (data not shown) indirectly, confirming that in endothelial cells, targeting of SR-BI to the plasma membrane does not depend on PDZK1.[40]

SR-BI has been shown to be involved in the protective effects of HDL on the endothelium, namely angiogenesis, migration, activation of endothelial nitric oxide synthase, and monocyte adhesion.[41] Recent studies have shown the association of enhanced expression of SR-BI expression in endothelial cells with decreased atherosclerosis in mice.[42] Thus, the requirement of VEGF on maintaining cell surface expression of SR-BI may have vascular effects beyond regulating transendothelial lipoprotein transport.

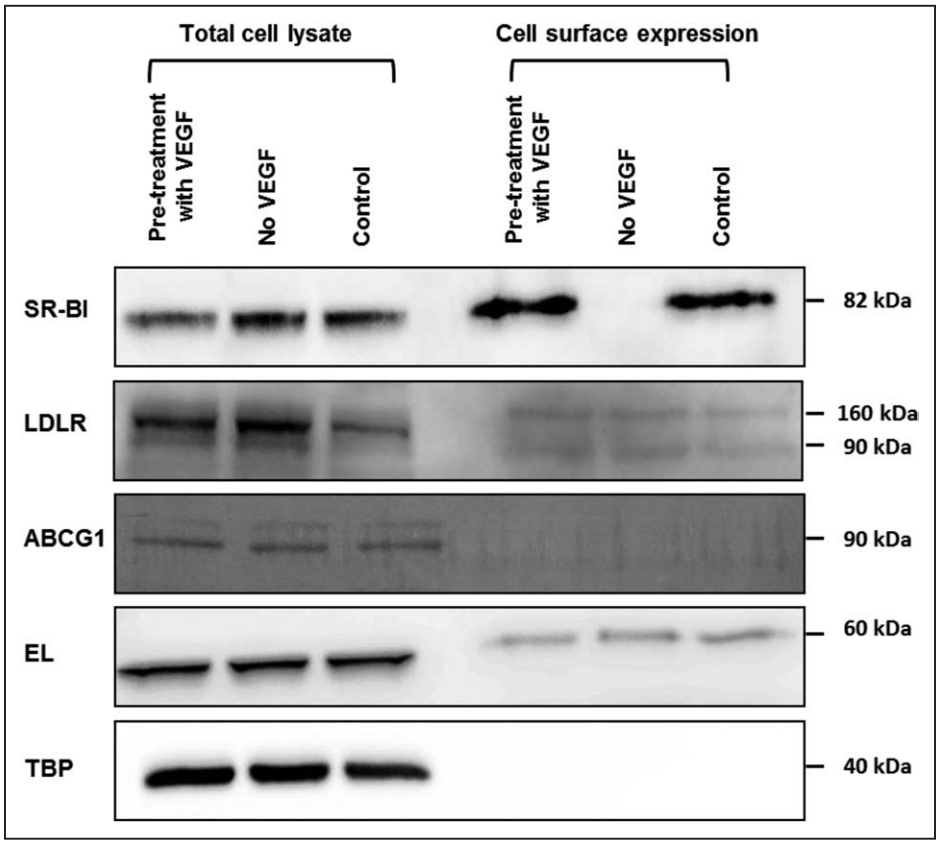

Figure 4. Vascular endothelial growth factor (VEGF)-A regulates cell surface expression of scavenger receptor BI (SR-BI). Western blots of SR-BI, low-density lipoprotein (LDL) receptor, ATP binding cassette transporter ABCG1, endothelial lipase (EL), and anti-TATA-binding protein (TBP) in total cell lysates (**left**) and on the cell surface (**right**). Human aortic endothelial cells (HAECs) were cultured in the presence or absence of VEGF for 72 hours, and cells were then pretreated with 25 ng/mL of $VEGF_{165}$ for 1 hour if indicated. The Western blot was probed with anti-SR-BI (82 kDa), anti-LDLR (95 and 160 kDa), anti-ABCG1 (90 kDa), as well as anti–endothelial lipase (EL; 60 kDa) and anti–TATA-binding protein (TBP; 40 kDa, as control for intracellular protein expression).

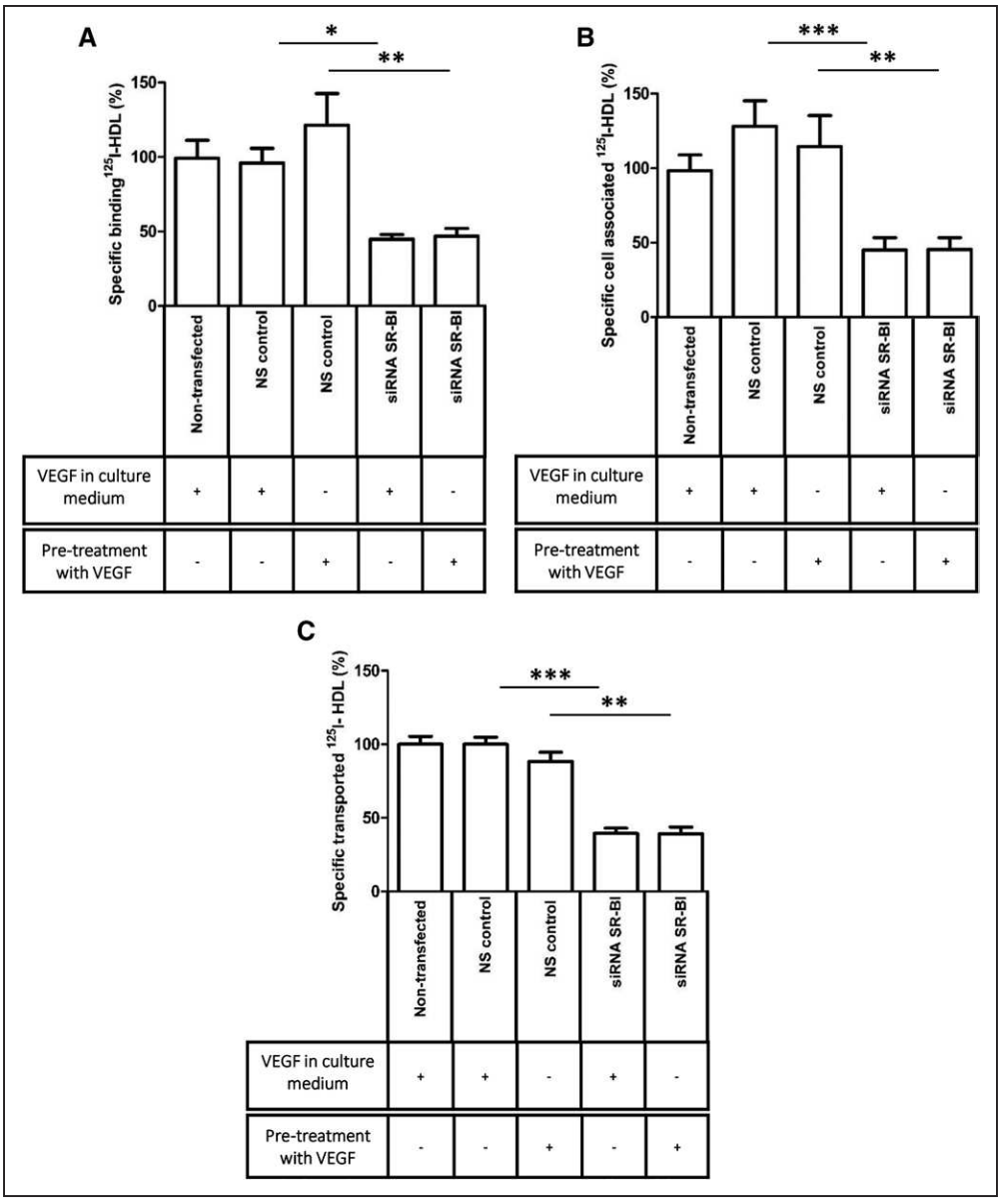

Figure 5. Vascular endothelial growth factor (VEGF)-A modulates scavenger receptor BI (SR-BI)–dependent binding, association, and transport of high-density lipoprotein (HDL) by human aortic endothelial cells (HAECs). HAECs were transfected with a specific siRNA against SR-BI or with nonsilencing control siRNA (NS control) in the presence or absence of VEGF-A-containing medium, and assays were performed 72 hours posttransfection. **A**, Specific binding was measured by incubating cells with ^{125}I-HDL at 4°C. **B**, Specific cell association was analyzed by incubating cells with ^{125}I-HDL at 37°C. **C**, ECs were cultured on inserts, and transport of ^{125}I-HDL from the apical to basolateral compartment was measured at 37°C. The results are represented as mean±SEM of 3 independent triplicate experiments (n=3). ***P≤0.001, **P≤0.01, *P≤0.05.

HDL was previously reported to enhance hypoxia-induced angiogenesis by stimulating the expression of VEGF and VEGFR2 in endothelial cells by a mechanism involving SR-BI.[43,44] It, thus, seems that in endothelial cells, HDL and SR-BI are both upstream regulators and downstream targets of the VEGF/VEGFR2 system.

We confirmed previous reports[3,10–13] that endothelial cells internalize and transcytose LDL. We also confirmed the previous report of Armstrong et al[12] that this process involves SR-BI (Velagapudi, Rohrer, von Eckardstein, unpublished observations). However, despite regulating the cell surface abundance of SR-BI, VEGF does not regulate the transendothelial transport of LDL. Neither the interference with the VEGF receptors by drugs or RNAi nor the removal or addition of VEGF had any significant effect on the binding, uptake, or transport of LDL by HAECs. These lipoprotein-specific effects of VEGF on the processing of HDL and LDL by HAECs indicate the existence of additional regulators and routes of transendothelial transport, for example, activin-like kinase 1, which was recently identified by a genome-wide RNAi-screen as an endothelial LDL-binding protein mediating uptake and transcytosis of LDL.[13]

From a more general perspective, our findings provide further evidence that transendothelial lipoprotein transport occurs by regulated processes[3,6–8,12,13] rather than passive filtration.[4] Dys-regulated transendothelial lipoprotein transport

may influence the pathogenesis of atherosclerosis beyond plasma levels of LDL and HDL. In fact, it was recently shown in LDL receptor–deficient mice that acute lowering of LDL cholesterol with anti-ApoB antisense oligonucleotides rapidly reduces the permeability of the aortic endothelium for LDL and causes regression of atherosclerosis independently of LDL pool size.[45] It is less obvious how changes in arterial permeability for HDL may affect atherosclerosis. At first sight, increased availability of HDL in the subendothelium will be protective, for example, by enhancing cholesterol efflux from macrophage foam cells. However, this will only be effective if HDL also leave the arterial wall to conclude reverse cholesterol transport. Disturbed egress of HDL from the arterial wall, potentially via the lymphatics,[24,25] will lead to the accumulation of HDL in the arterial wall. These particles will be eventually oxidized and become dysfunctional[46,47] and, thereby, promote rather than inhibit cholesterol accumulation and, hence, atherosclerosis.

In conclusion, we here showed that the VEGF-A/VEGFR2 regulates endothelial binding, uptake, and transport of HDL through PI3K/Akt and p38 MAPK and, as the final result, cell surface expression of SR-BI. Thereby, VEGF-A may play an important regulatory role for the vascular protective effects of HDL, as well as reverse cholesterol transport.

Acknowledgments

We thank Silvija Radosavljevic and Miriam Degen Steiner for their technical assistance.

Sources of Funding

This work was supported by grants from the Zurich Integrative Human Physiology and Swiss National Science Foundation (31003A-160126) and the 7th Framework Program of the European Commission (TransCard; project number 603091).

Disclosures

None.

References

1. Borén J, Williams KJ. The central role of arterial retention of cholesterol-rich apolipoprotein-B-containing lipoproteins in the pathogenesis of atherosclerosis: a triumph of simplicity. *Curr Opin Lipidol*. 2016;27:473–483. doi: 10.1097/MOL.0000000000000330.
2. von Eckardstein A, Rohrer L. HDLs in crises. *Curr Opin Lipidol*. 2016;27:264–273. doi: 10.1097/MOL.0000000000000294.
3. von Eckardstein A, Rohrer L. Transendothelial lipoprotein transport and regulation of endothelial permeability and integrity by lipoproteins. *Curr Opin Lipidol*. 2009;20:197–205. doi: 10.1097/MOL.0b013e32832afd63.
4. Michel CC, Nanjee MN, Olszewski WL, Miller NE. LDL and HDL transfer rates across peripheral microvascular endothelium agree with those predicted for passive ultrafiltration in humans. *J Lipid Res*. 2015;56:122–128. doi: 10.1194/jlr.M055053.
5. Perisa D, Rohrer L, Kaech A, von Eckardstein A. Itinerary of high density lipoproteins in endothelial cells. *Biochim Biophys Acta*. 2016;1861:98–107. doi: 10.1016/j.bbalip.2015.11.004.
6. Rohrer L, Ohnsorg PM, Lehner M, Landolt F, Rinninger F, von Eckardstein A. High-density lipoprotein transport through aortic endothelial cells involves scavenger receptor BI and ATP-binding cassette transporter G1. *Circ Res*. 2009;104:1142–1150. doi: 10.1161/CIRCRESAHA.108.190587.
7. Robert J, Lehner M, Frank S, Perisa D, von Eckardstein A, Rohrer L. Interleukin 6 stimulates endothelial binding and transport of high-density lipoprotein through induction of endothelial lipase. *Arterioscler Thromb Vasc Biol*. 2013;33:2699–2706. doi: 10.1161/ATVBAHA.113.301363.
8. Cavelier C, Ohnsorg PM, Rohrer L, von Eckardstein A. The β-chain of cell surface F(0)F(1) ATPase modulates apoA-I and HDL transcytosis through aortic endothelial cells. *Arterioscler Thromb Vasc Biol*. 2012;32:131–139. doi: 10.1161/ATVBAHA.111.238063.
9. Goldstein JL, Brown MS. The LDL receptor. *Arterioscler Thromb Vasc Biol*. 2009;29:431–438. doi: 10.1161/ATVBAHA.108.179564.
10. Vasile E, Simionescu M, Simionescu N. Visualization of the binding, endocytosis, and transcytosis of low-density lipoprotein in the arterial endothelium in situ. *J Cell Biol*. 1983;96:1677–1689.
11. Pavlides S, Gutierrez-Pajares JL, Iturrieta J, Lisanti MP, Frank PG. Endothelial caveolin-1 plays a major role in the development of atherosclerosis. *Cell Tissue Res*. 2014;356:147–157. doi: 10.1007/s00441-013-1767-7.
12. Armstrong SM, Sugiyama MG, Fung KY, et al. A novel assay uncovers an unexpected role for SR-BI in LDL transcytosis. *Cardiovasc Res*. 2015;108:268–277. doi: 10.1093/cvr/cvv218.
13. Kraehling JR, Chidlow JH, Rajagopal C, et al. Genome-wide RNAi screen reveals ALK1 mediates LDL uptake and transcytosis in endothelial cells. *Nat Commun*. 2016;7:13516. doi: 10.1038/ncomms13516.
14. Pelkmans L, Fava E, Grabner H, Hannus M, Habermann B, Krausz E, Zerial M. Genome-wide analysis of human kinases in clathrin- and caveolae/raft-mediated endocytosis. *Nature*. 2005;436:78–86. doi: 10.1038/nature03571.
15. Lu D, Kussie P, Pytowski B, Persaud K, Bohlen P, Witte L, Zhu Z. Identification of the residues in the extracellular region of KDR important for interaction with vascular endothelial growth factor and neutralizing anti-KDR antibodies. *J Biol Chem*. 2000;275:14321–14330.
16. Millauer B, Wizigmann-Voos S, Schnürch H, Martinez R, Møller NP, Risau W, Ullrich A. High affinity VEGF binding and developmental expression suggest Flk-1 as a major regulator of vasculogenesis and angiogenesis. *Cell*. 1993;72:835–846.
17. Quinn TP, Peters KG, De Vries C, Ferrara N, Williams LT. Fetal liver kinase 1 is a receptor for vascular endothelial growth factor and is selectively expressed in vascular endothelium. *Proc Natl Acad Sci U S A*. 1993;90:7533–7537.
18. Olofsson B, Korpelainen E, Pepper MS, Mandriota SJ, Aase K, Kumar V, Gunji Y, Jeltsch MM, Shibuya M, Alitalo K, Eriksson U. Vascular endothelial growth factor B (VEGF-B) binds to VEGF receptor-1 and regulates plasminogen activator activity in endothelial cells. *Proc Natl Acad Sci U S A*. 1998;95:11709–11714.
19. Park JE, Chen HH, Winer J, Houck KA, Ferrara N. Placenta growth factor. Potentiation of vascular endothelial growth factor bioactivity, *in vitro* and in vivo, and high affinity binding to Flt-1 but not to Flk-1/KDR. *J Biol Chem*. 1994;269:25646–25654.
20. Terman BI, Dougher-Vermazen M, Carrion ME, Dimitrov D, Armellino DC, Gospodarowicz D, Böhlen P. Identification of the KDR tyrosine kinase as a receptor for vascular endothelial cell growth factor. *Biochem Biophys Res Commun*. 1992;187:1579–1586.
21. Joukov V, Pajusola K, Kaipainen A, Chilov D, Lahtinen I, Kukk E, Saksela O, Kalkkinen N, Alitalo K. A novel vascular endothelial growth factor, VEGF-C, is a ligand for the Flt4 (VEGFR-3) and KDR (VEGFR-2) receptor tyrosine kinases. *EMBO J*. 1996;15:290–298.
22. Achen MG, Jeltsch M, Kukk E, Mäkinen T, Vitali A, Wilks AF, Alitalo K, Stacker SA. Vascular endothelial growth factor D (VEGF-D) is a ligand for the tyrosine kinases VEGF receptor 2 (Flk1) and VEGF receptor 3 (Flt4). *Proc Natl Acad Sci U S A*. 1998;95:548–553.
23. Kappas NC, Zeng G, Chappell JC, Kearney JB, Hazarika S, Kallianos KG, Patterson C, Annex BH, Bautch VL. The VEGF receptor Flt-1 spatially modulates Flk-1 signaling and blood vessel branching. *J Cell Biol*. 2008;181:847–858. doi: 10.1083/jcb.200709114.
24. Lim HY, Thiam CH, Yeo KP, Bisoendial R, Hii CS, McGrath KC, Tan KW, Heather A, Alexander JS, Angeli V. Lymphatic vessels are essential for the removal of cholesterol from peripheral tissues by SR-BI-mediated transport of HDL. *Cell Metab*. 2013;17:671–684. doi: 10.1016/j.cmet.2013.04.002.
25. Martel C, Li W, Fulp B, Platt AM, Gautier EL, Westerterp M, Bittman R, Tall AR, Chen SH, Thomas MJ, Kreisel D, Swartz MA, Sorci-Thomas MG, Randolph GJ. Lymphatic vasculature mediates macrophage reverse cholesterol transport in mice. *J Clin Invest*. 2013;123:1571–1579. doi: 10.1172/JCI63685.
26. Waltenberger J, Claesson-Welsh L, Siegbahn A, Shibuya M, Heldin CH. Different signal transduction properties of KDR and Flt1, two receptors for vascular endothelial growth factor. *J Biol Chem*. 1994;269:26988–26995.
27. Takahashi T, Shibuya M. The 230 kDa mature form of KDR/Flk-1 (VEGF receptor-2) activates the PLC-gamma pathway and partially induces

mitotic signals in NIH3T3 fibroblasts. *Oncogene*. 1997;14:2079–2089. doi: 10.1038/sj.onc.1201047.
28. Igarashi K, Isohara T, Kato T, Shigeta K, Yamano T, Uno I. Tyrosine 1213 of Flt-1 is a major binding site of Nck and SHP-2. *Biochem Biophys Res Commun*. 1998;246:95–99. doi: 10.1006/bbrc.1998.8578.
29. Guo D, Jia Q, Song HY, Warren RS, Donner DB. Vascular endothelial cell growth factor promotes tyrosine phosphorylation of mediators of signal transduction that contain SH2 domains. Association with endothelial cell proliferation. *J Biol Chem*. 1995;270:6729–6733.
30. Lamalice L, Houle F, Jourdan G, Huot J. Phosphorylation of tyrosine 1214 on VEGFR2 is required for VEGF-induced activation of Cdc42 upstream of SAPK2/p38. *Oncogene*. 2004;23:434–445. doi: 10.1038/sj.onc.1207034.
31. Backer JM. Phosphoinositide 3-kinases and the regulation of vesicular trafficking. *Mol Cell Biol Res Commun*. 2000;3:193–204. doi: 10.1006/mcbr.2000.0202.
32. Corvera S. Phosphatidylinositol 3-kinase and the control of endosome dynamics: new players defined by structural motifs. *Traffic*. 2001;2:859–866.
33. Hansen SH, Olsson A, Casanova JE. Wortmannin, an inhibitor of phosphoinositide 3-kinase, inhibits transcytosis in polarized epithelial cells. *J Biol Chem*. 1995;270:28425–28432.
34. van Dam EM, Govers R, James DE. Akt activation is required at a late stage of insulin-induced GLUT4 translocation to the plasma membrane. *Mol Endocrinol*. 2005;19:1067–1077. doi: 10.1210/me.2004-0413.
35. Shetty S, Eckhardt ER, Post SR, van der Westhuyzen DR. Phosphatidylinositol-3-kinase regulates scavenger receptor class B type I subcellular localization and selective lipid uptake in hepatocytes. *Arterioscler Thromb Vasc Biol*. 2006;26:2125–2131. doi: 10.1161/01.ATV.0000233335.26362.37.
36. Rousseau S, Houle F, Kotanides H, Witte L, Waltenberger J, Landry J, Huot J. Vascular endothelial growth factor (VEGF)-driven actin-based motility is mediated by VEGFR2 and requires concerted activation of stress-activated protein kinase 2 (SAPK2/p38) and geldanamycin-sensitive phosphorylation of focal adhesion kinase. *J Biol Chem*. 2000;275:10661–10672.
37. Rousseau S, Houle F, Landry J, Huot J. p38 MAP kinase activation by vascular endothelial growth factor mediates actin reorganization and cell migration in human endothelial cells. *Oncogene*. 1997;15:2169–2177. doi: 10.1038/sj.onc.1201380.
38. Tondu AL, Robichon C, Yvan-Charvet L, Donne N, Le Liepvre X, Hajduch E, Ferré P, Dugail I, Dagher G. Insulin and angiotensin II induce the translocation of scavenger receptor class B, type I from intracellular sites to the plasma membrane of adipocytes. *J Biol Chem*. 2005;280:33536–33540. doi: 10.1074/jbc.M502392200.
39. Silver DL. A carboxyl-terminal PDZ-interacting domain of scavenger receptor B, type I is essential for cell surface expression in liver. *J Biol Chem*. 2002;277:34042–34047. doi: 10.1074/jbc.M206584200.
40. Zhu W, Saddar S, Seetharam D, Chambliss KL, Longoria C, Silver DL, Yuhanna IS, Shaul PW, Mineo C. The scavenger receptor class B type I adaptor protein PDZK1 maintains endothelial monolayer integrity. *Circ Res*. 2008;102:480–487. doi: 10.1161/CIRCRESAHA.107.159079.
41. Trigatti BL, Krieger M, Rigotti A. Influence of the HDL receptor SR-BI on lipoprotein metabolism and atherosclerosis. *Arterioscler Thromb Vasc Biol*. 2003;23:1732–1738. doi: 10.1161/01.ATV.0000091363.28501.84.
42. Vaisman BL, Vishnyakova TG, Freeman LA, Amar MJ, Demosky SJ, Liu C, Stonik JA, Sampson ML, Pryor M, Bocharov AV, Eggerman TL, Patterson AP, Remaley AT. Endothelial Expression of Scavenger Receptor Class B, Type I Protects against Development of Atherosclerosis in Mice. *Biomed Res Int*. 2015;2015:607120. doi: 10.1155/2015/607120.
43. Tan JT, Prosser HC, Dunn LL, Vanags LZ, Ridiandries A, Tsatralis T, Leece L, Clayton ZE, Yuen SC, Robertson S, Lam YT, Celermajer DS, Ng MK, Bursill CA. High-density lipoproteins rescue diabetes-impaired angiogenesis via scavenger receptor class B type I. *Diabetes*. 2016;65:3091–3103. doi: 10.2337/db15-1668.
44. Prosser HC, Tan JT, Dunn LL, Patel S, Vanags LZ, Bao S, Ng MK, Bursill CA. Multifunctional regulation of angiogenesis by high-density lipoproteins. *Cardiovasc Res*. 2014;101:145–154. doi: 10.1093/cvr/cvt234.
45. Bartels ED, Christoffersen C, Lindholm MW, Nielsen LB. Altered metabolism of LDL in the arterial wall precedes atherosclerosis regression. *Circ Res*. 2015;117(11):933–942.
46. Huang Y, DiDonato JA, Levison BS, et al. An abundant dysfunctional apolipoprotein A1 in human atheroma. *Nat Med*. 2014;20:193–203. doi: 10.1038/nm.3459.
47. DiDonato JA, Aulak K, Huang Y, Wagner M, Gerstenecker G, Topbas C, Gogonea V, DiDonato AJ, Tang WH, Mehl RA, Fox PL, Plow EF, Smith JD, Fisher EA, Hazen SL. Site-specific nitration of apolipoprotein A-I at tyrosine 166 is both abundant within human atherosclerotic plaque and dysfunctional. *J Biol Chem*. 2014;289:10276–10292. doi: 10.1074/jbc.M114.556506.

Highlights

- Vascular endothelial growth factor (VEGF)-A stimulates the binding, uptake, and transcellular transport of high-density lipoprotein but not low-density lipoprotein by aortic endothelial cells.
- These stimulatory effects of VEGF-A require VEGF receptor 2 but neither VEGF receptor 1 nor VEGF receptor 3.
- These stimulatory effects of VEGF-A involve phosphatidyl-inositol 3 kinase/protein kinase B and p38 mitogen-activated protein kinase as well as scavenger receptor BI.
- VEGF-A stimulates the translocation of scavenger receptor BI to the plasma membrane.

Arteriosclerosis, Thrombosis, and Vascular Biology

JOURNAL OF THE AMERICAN HEART ASSOCIATION

VEGF-A Regulates Cellular Localization of SR-BI as Well as Transendothelial Transport of HDL but Not LDL

Srividya Velagapudi, Mustafa Yalcinkaya, Antonio Piemontese, Roger Meier, Simon Flyvbjerg Nørrelykke, Damir Perisa, Andrzej Rzepiela, Michael Stebler, Szymon Stoma, Paolo Zanoni, Lucia Rohrer and Arnold von Eckardstein

Arterioscler Thromb Vasc Biol. 2017;37:794-803; originally published online March 30, 2017; doi: 10.1161/ATVBAHA.117.309284

Arteriosclerosis, Thrombosis, and Vascular Biology is published by the American Heart Association, 7272 Greenville Avenue, Dallas, TX 75231

Print ISSN: 1079-5642. Online ISSN: 1524-4636

VEGF-A regulates subcellular localization of scavenger receptor BI and transcytosis of HDL but not LDL in aortic endothelial cells

Srividya Velagapudi, M.Sc[1,2], Mustafa Yalcinkaya, M.Sc[1,2] , Antonio Piemontese, PhD[1,3], Roger Meier, PhD[4], Simon Flyvbjerg Nørrelykke, PhD[4] , Damir Perisa, PhD[1,2], Andrzej Rzepiela, PhD[4], Michael Stebler, M.Sc[4], Szymon Stoma, PhD[4], Paolo Zanoni, MD[1,2], Lucia Rohrer, PhD[1,2,*], and Arnold von Eckardstein, MD[1,2,*]

Supplement Material

Supplementary Figure I

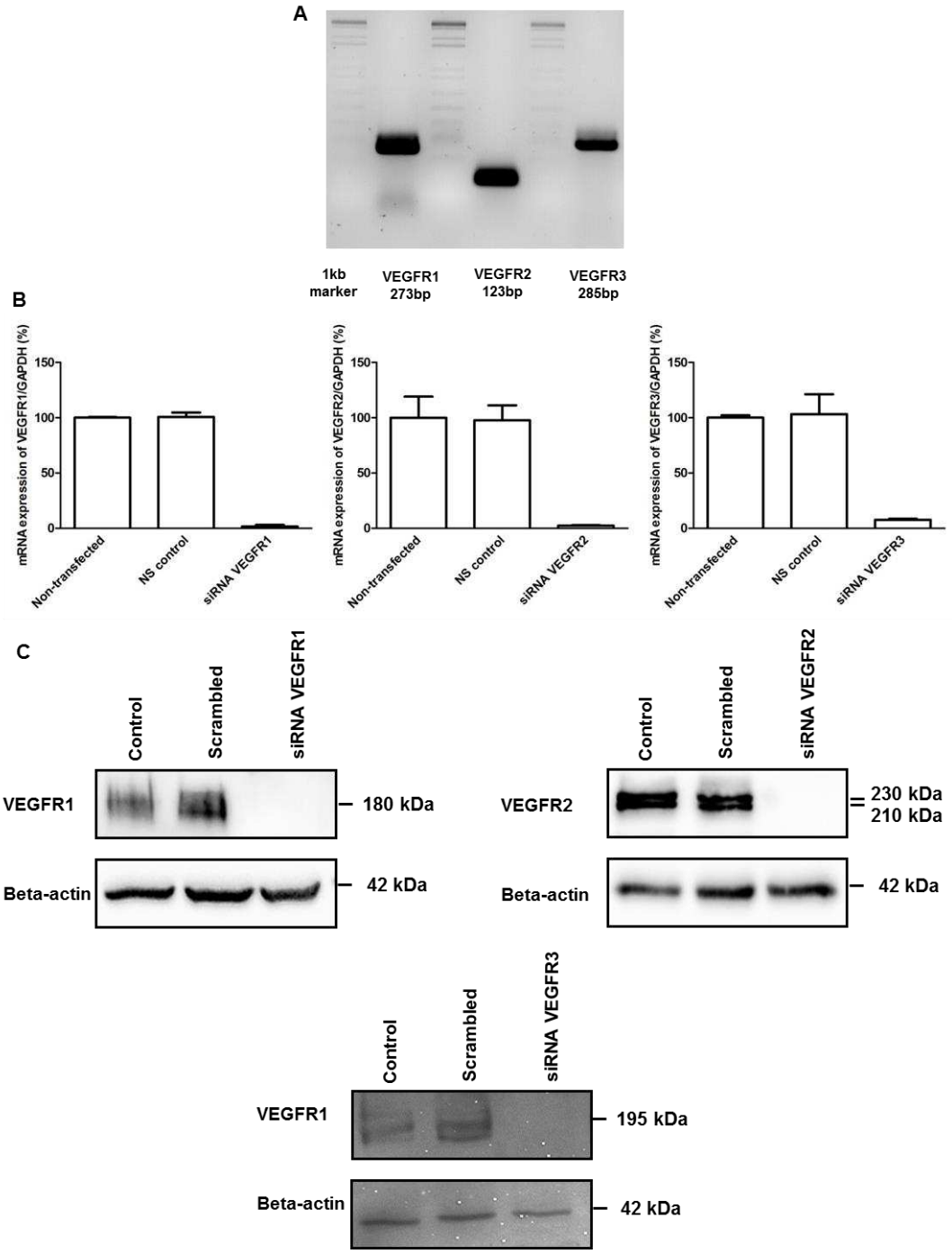

Supplementary Figure I: Expression of VEGF receptors (A) and efficiency of RNA interference (B, C)

A, mRNA levels of VEGFR1, VEGFR2 and VEGFR3 in HAECs were measured by real-time polymerase chain reaction. HAECs were transfected with specific siRNA against VEGFR1, VEGFR2, or VEGFR3 or with non-silencing control siRNA (NS control). Assays were performed 72hours after transfection. Silencing efficiency was analyzed at the **B,** mRNA level using qRT-PCR and **C,** protein level using western blotting. The western blots were probed with antibodies against VEGFR1 (180 kDa), VEGFR2 (210 kDa, 230 kDa) and VEGFR3 (195 kDa) respectively and Beta-actin (42 kDa) was used as the loading control.

Supplementary Figure II

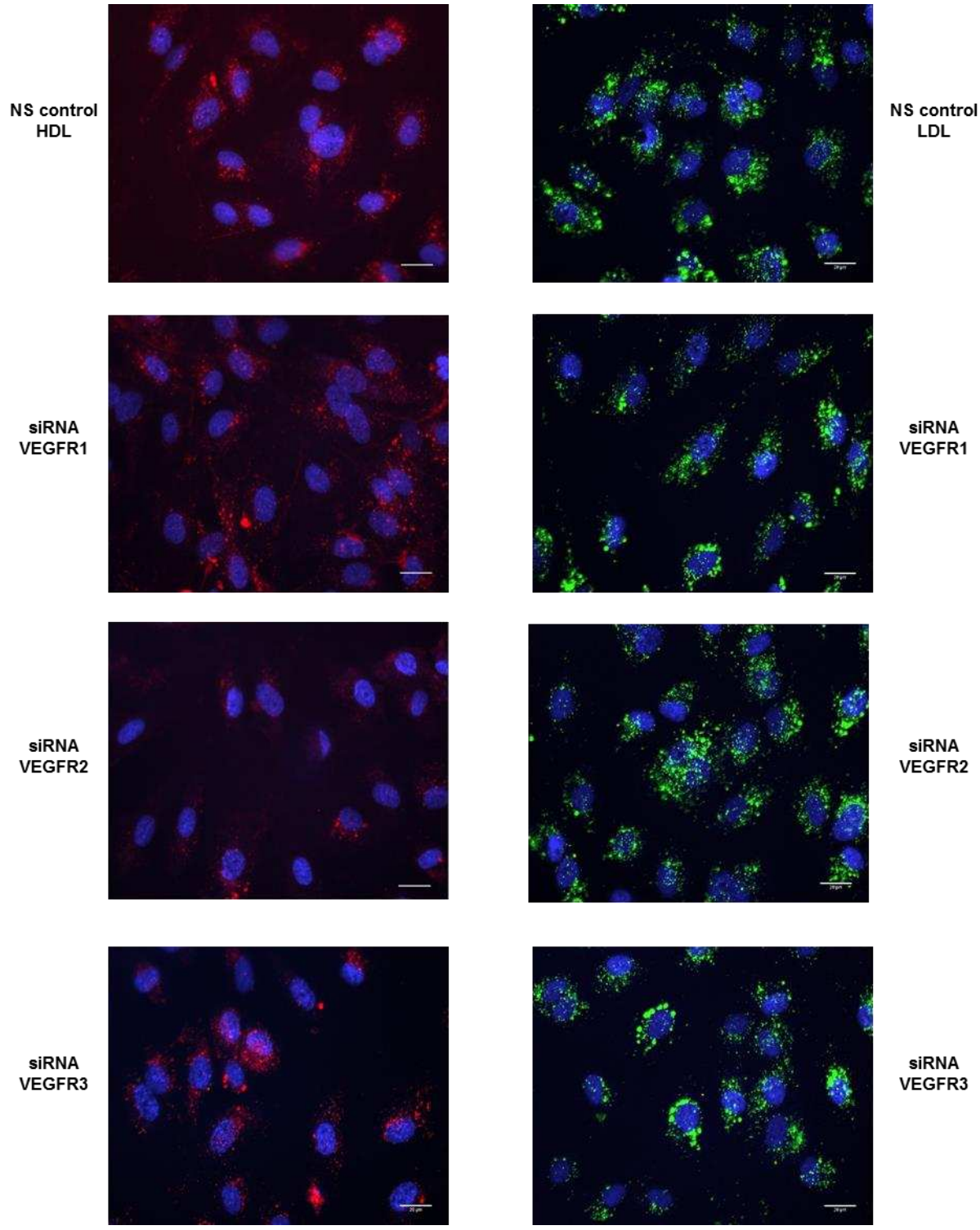

Supplementary Figure II: Effect of VEGF receptors on the uptake of HDL (left lane) and LDL (right lane) by HAECs

HAECs were transfected with a specific siRNA against VEGFR2 or with non-silencing control siRNA (NS control) and fluorescent lipoprotein uptake assay was performed 72hours after transfection. Uptake of Atto594-HDL (red) and Atto488-LDL (green) into transfected endothelial cells was analyzed by wide-field fluorescence microscopy. ECs were incubated with 50ug/ml of Atto594-HDL or 50ug/ml Atto488-LDL for 1hour prior to fixation and nuclei were counterstained with DAPI (blue). Scale bar is 20µM.

Supplementary Figure III

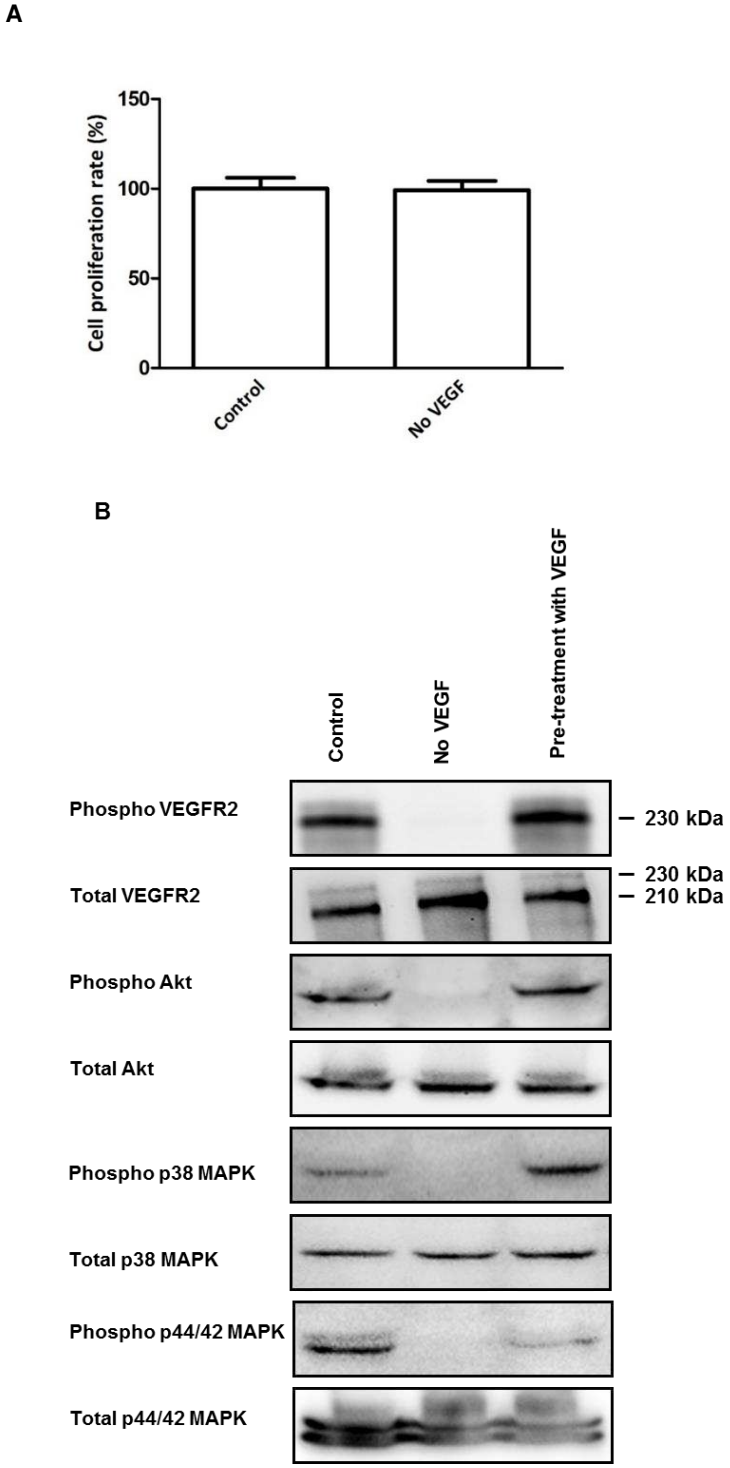

Supplementary Figure III: Effect of VEGF-A on HAECs proliferation (A) and phosphorylation of VEGFR2 and its downstream kinases (B). HAECs were cultured in regular medium containing VEGF-A (control) or in medium free of VEGF-A (no VEGF) for 72hours or cells were pre-treated with 25ng/ml of $VEGF_{165}$ for 1hour prior to protein extraction. **A:** The rate of cell proliferation was analyzed using the MTT assay. The results are representative of three individual experiments (n=3). **B:** Cell lysates were analysed by western blotting for phospho VEGFR2 (Tyrosine 1054/1059) and total VEGFR2, phospho Akt (Ser-473) and total Akt, phospho p38 MAPK (Thr180/Tyr182) and total p38 MAPK, phospho ERK1/2 (Thr202/Tyr204 & Thr185/Tyr187) and total ERK1/2

Supplementary Figure IV

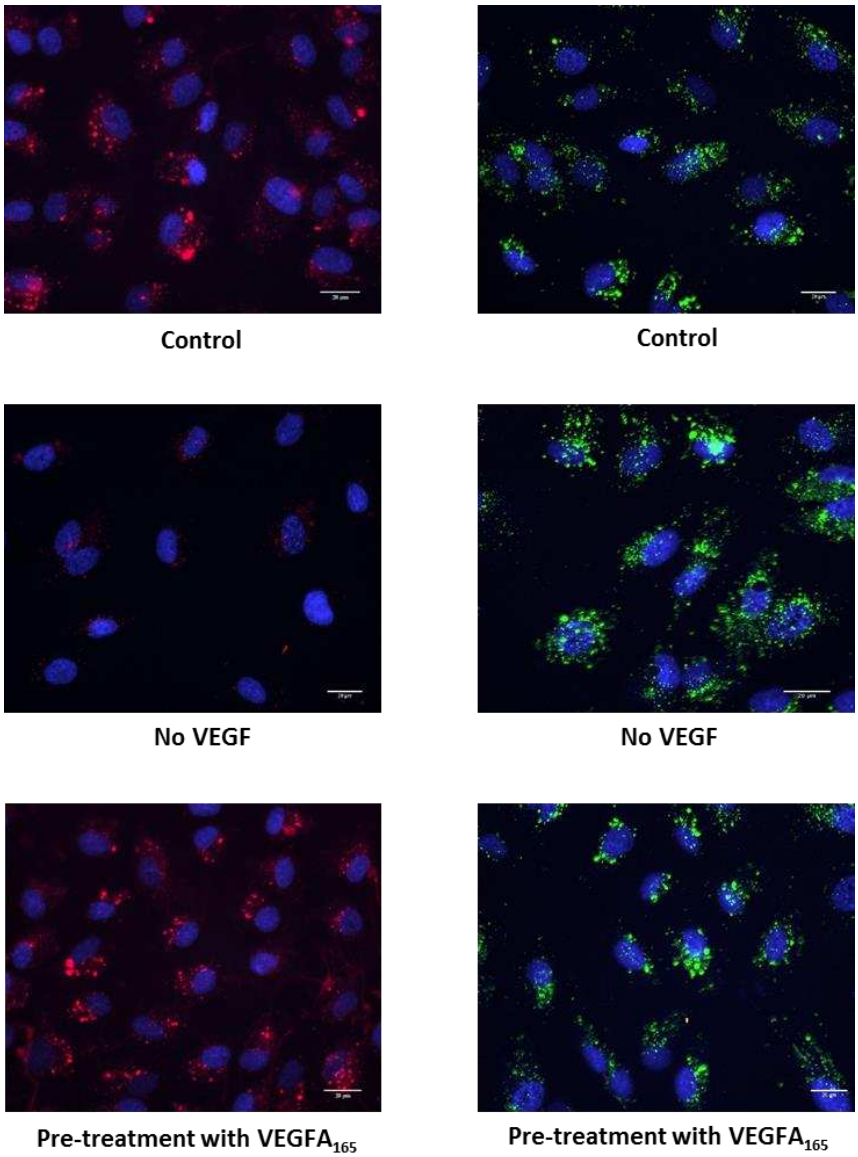

Supplementary Figure IV: Effect of VEGF-A treatment on HDL (left lane) and LDL (right lane) uptake by HAECs

HAECs were cultured in the presence of VEGF-A (control) or absence of VEGF-A (no VEGF) for 72hours or cells were pre-treated with 25ng/ml of $VEGF_{165}$ for 1hour prior to the incubation with fluorescent lipoproteins. ECs were incubated with 50ug/ml of Atto594-HDL or Atto488-LDL for 1hour prior to fixation and nuclei were counterstained with DAPI (blue). Uptake of Atto594-HDL (red) and Atto488-LDL (green) in endothelial cells was analyzed by wide-field microscopy. Scale bar is 20µM.

Supplementary Figure V

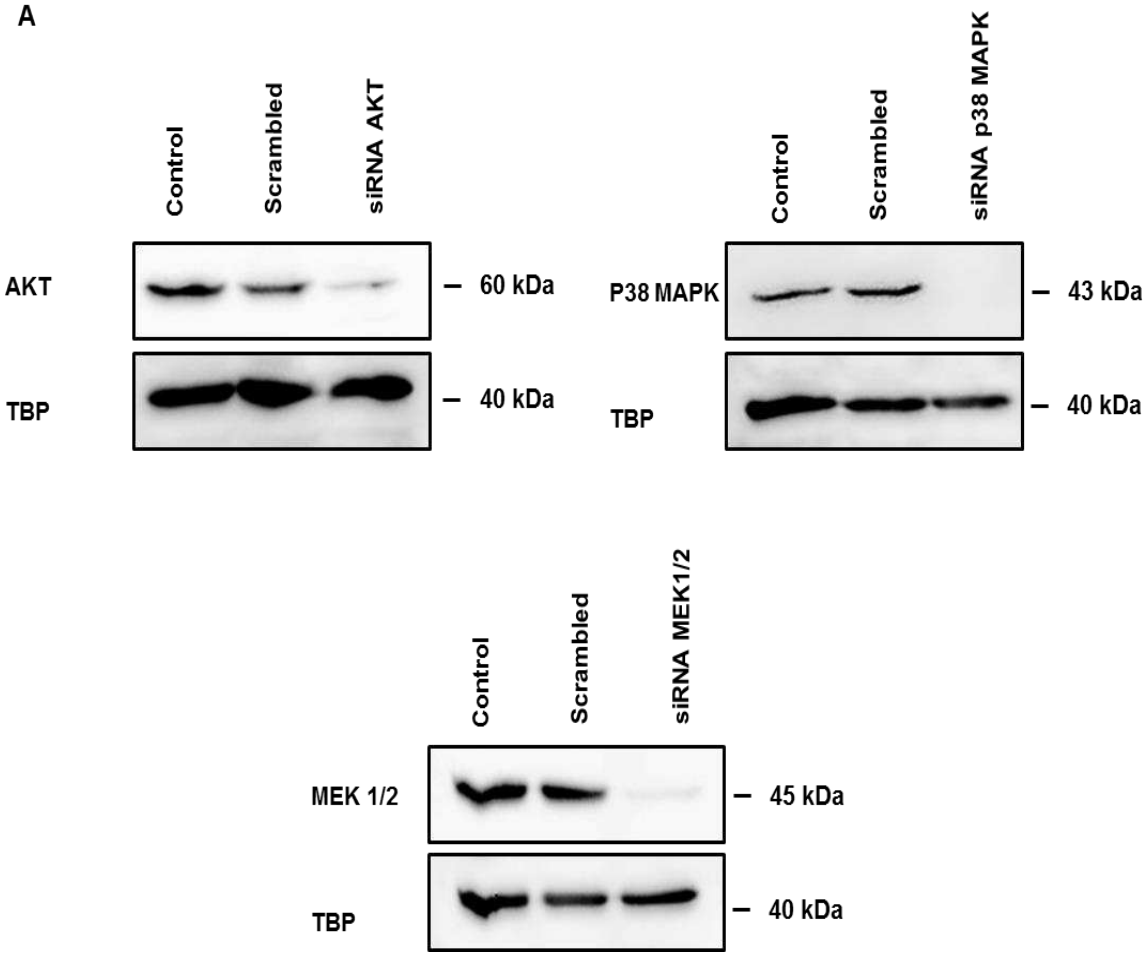

Supplementary Figure V: Silencing efficiency of AKT, p38 MAPK and MEK1/2
Protein levels of Akt, p38 MAPK and MEK1/2 were measured using western blotting following transfection of ECs with specific siRNAs against AKT, MAPK14 (p38 MAPK), MAP2K1/MAP2K2 (MEK1/2). TATA-binding protein (TBP) was used as a loading control.

Supplementary Figure VI

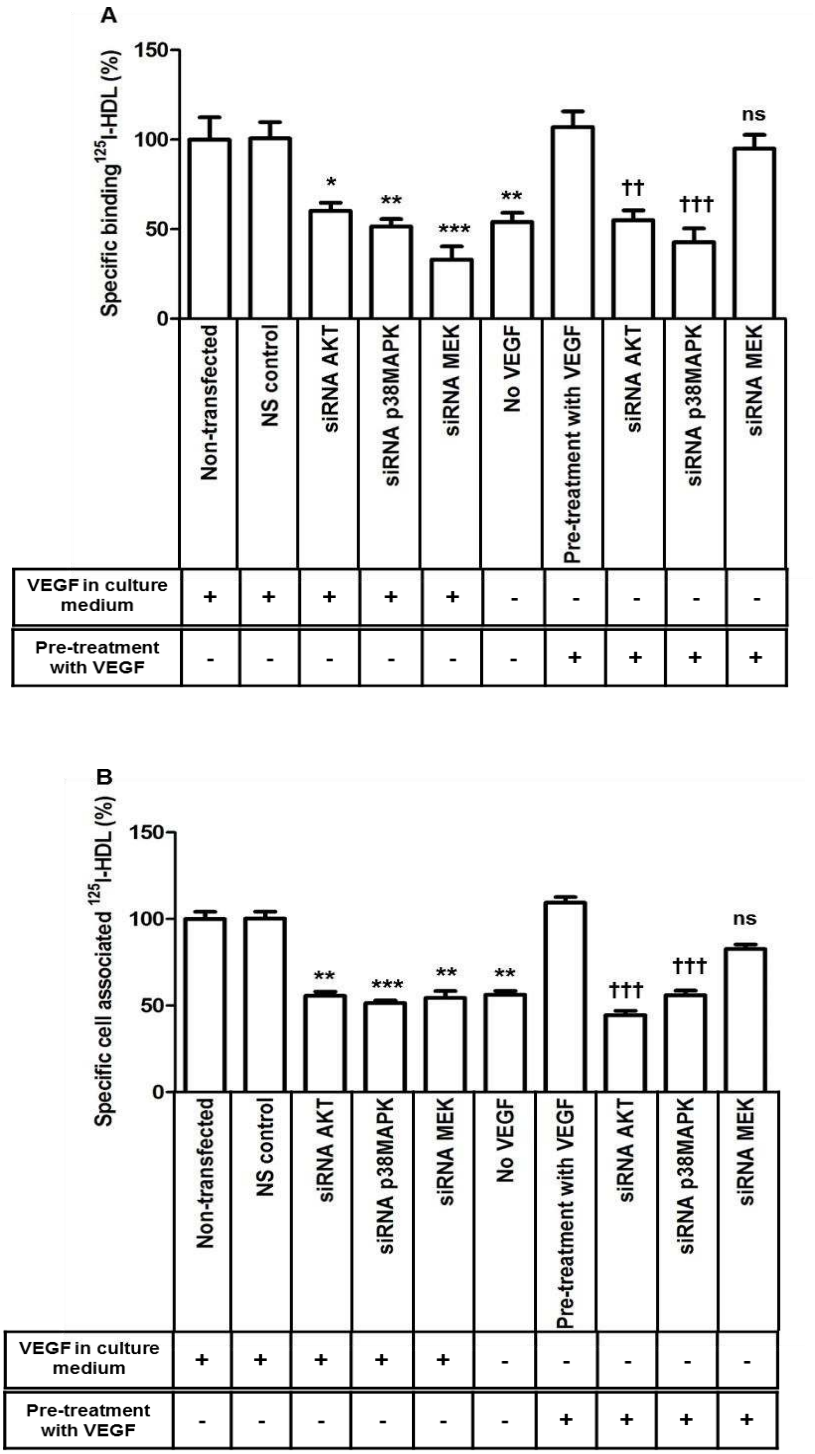

Supplementary Figure VI: VEGF-A regulates HDL binding and association through PI3K/Akt and p38 MAPK

HAECs were transfected with specific siRNA against AKT or MAPK14 (p38 MAPK) or MAP2K1/MAP2K2 (MEK1/2) or with non-silencing control (NS control) siRNA in the presence or absence of VEGF-A containing medium and assays were performed 72hours post-transfection. **A**, Specific binding was measured by incubating cells with ^{125}I-HDL at 4 ºC. **B**, Specific cell association was analyzed by incubating cells with ^{125}I-HDL at 37 ºC. The results are represented as mean±SEM and three independent triplicate experiments (n=3). ***$P \leq 0.001$, **$P \leq 0.01$, *$P \leq 0.05$

†††$P \leq 0.001$, ††$P \leq 0.01$, †$P \leq 0.05$ and ns represents "not significant"

Supplementary Figure VII

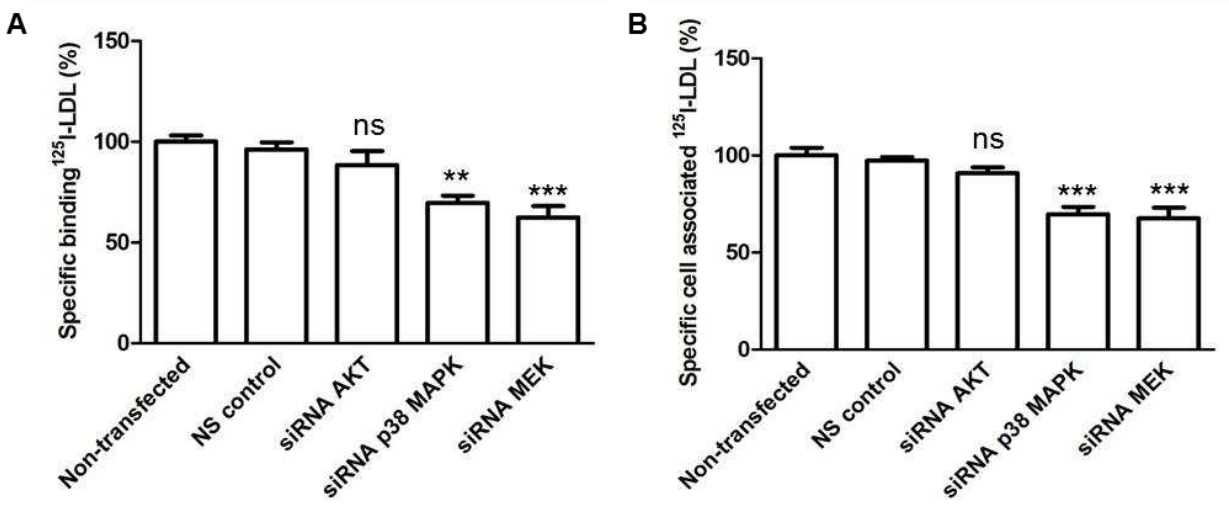

Supplementary Figure VII: Binding and association of ^{125}I-LDL through p38 MAPK and MEK1/2
HAECs were transfected with specific siRNA against AKT or MAPK14 (p38 MAPK) or MAP2K1/MAP2K2 (MEK1/2) or with non-silencing control (NS control) siRNA in the presence of VEGF-A containing medium and assays were performed 72hours post-transfection. **A**, Specific binding was measured by incubating cells with ^{125}I-LDL at 4 ºC. **B**, Specific cell association was analyzed by incubating cells with ^{125}I-LDL at 37 ºC. The results are represented as mean±SEM and three independent triplicate experiments (n=3). ****P*≤ 0.001, ***P*≤ 0.01, **P*≤ 0.05 and ns represents "not significant"

Supplementary Figure VIII

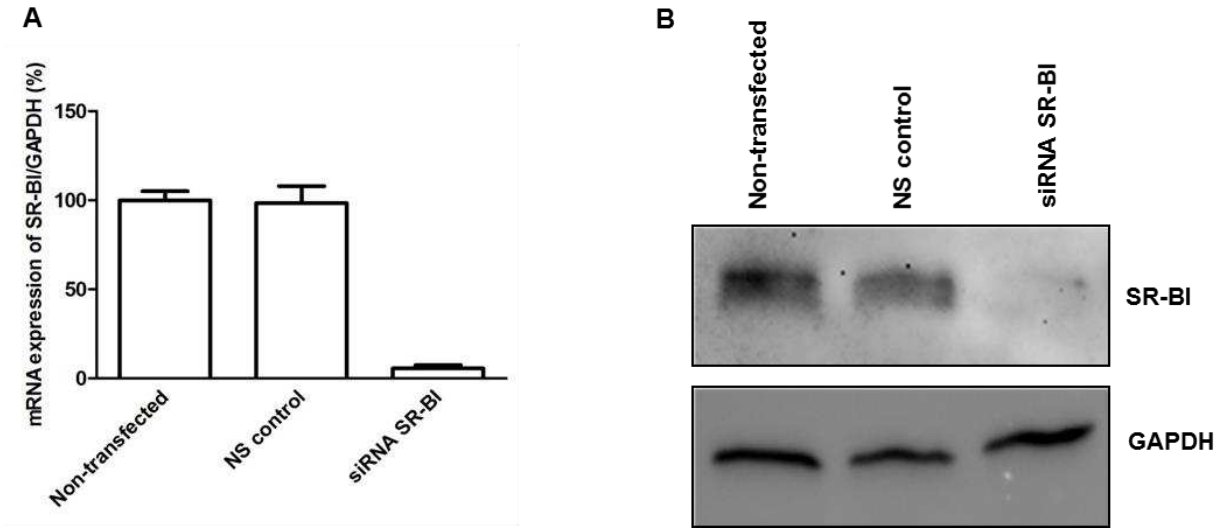

Supplementary Figure VIII: Efficiency of silencing SR-BI
A, mRNA levels of SR-BI were analyzed following transfection of ECs with specific siRNAs against SR-BI. GAPDH was used as a housekeeping control. **B**, SR-BI (82 kDa) protein expression levels measured by western blotting, GAPDH (38 kDa) used as loading control.

Supplementary Tables

Supplementary Table I: List of kinase drug inhibitors used in the drug screening to study their effect on Atto 594-LDL cellular uptake in HAECs. For each drug interaction, nHill represents the Hill coefficient for the curve which is the measure of the slope at IC_{50}, qualified AC50 (qAC50) represents a reliable value based on computed IC_{50}, median residual activity was calculated relative to a control reaction in the presence of vehicle (DMSO) and standard error of the residual activity at the maximal drug concentration, represents a measure of screen reproducibility.

Supplementary Table II: List of kinase drug inhibitors used in the drug screening to study their effect on Atto 594-HDL cellular uptake in HAECs. For each drug interaction, nHill represents the Hill coefficient for the curve which is the measure of the slope at IC_{50}, qualified AC50 (qAC50) represents a reliable value based on computed IC_{50}, median residual activity was calculated relative to a control reaction in the presence of vehicle (DMSO) and standard error of the residual activity at the maximal drug concentration, represents a measure of screen reproducibility.

Supplementary Table I

Compound	CAS number	Target	nHill	qAC50	Residual activity (Median)	Standard error
ABT-869(Linifanib)	796967-16-3	VEGFR	Inactive	0.005328	104.44	2.534
AC-220	950769-58-1	FLT-3	Inactive	0.003567	95.78	1.451
AEE788	497839-62-0	EGFR | HER1/2 | VEGFR | Flt-1	Inactive	0.004539	64.81	2.337
AG-490	133550-30-8	EGFR | JAK	Inactive	0.006796	73.27	3.79
AP24534	943319-70-8	VEGFR | FGFR | FLT-3	Inactive	0.000751	85.12	4.951
AS-605240	648450-29-7	PI3K	Inactive	0.007774	113.43	2.486
AS703026	1236699-92-5	MEK	Inactive	0.004638	117.35	2.297
AT7519	844442-38-2	CDK	Inactive	0.005232	109.26	0.9898
AT7867	857531-00-1	Akt	Inactive	0.00592	69.82	4.245
AT9283	896466-04-9	Aurora | JAK | ABL	4	0.005243	53.86	1.961
Aurora A Inhibitor I	1158838-45-9	Aurora	Inactive	0.003401	98.29	4.403
AV-951(Tivozanib)	475108-18-0	VEGFR	Inactive	0.004397	61.33	2.864
Axitinib	319460-85-0	VEGFR	Inactive	0.005175	95.89	1.096
AZD0530(Saracatinib)	379231-04-6	ABL	Inactive	0.00369	83.31	1.971
AZD1152-HQPA(Barasertib)	722544-51-6	Aurora	Inactive	0.00394	107.66	0.8166
AZD1480	935666-88-9	JAK	Inactive	0.005735	122.35	2.616
AZD6244(Selumetinib)	606143-52-6	MEK	Inactive	0.00437	108.08	2.115
AZD6482	1173900-33-8	PI3K	Inactive	0.004897	118.33	1.417
AZD7762	860352-01-8	CHK	Inactive	0.005518	100.01	1.221
AZD8055	1009298-09-2	mTOR	Inactive	0.004296	99.19	1.278
AZD8330	869357-68-6	MEK	Inactive	0.004336	106.09	1.822
BAY 73-4506(Regorafenib)	755037-03-7	c-KIT | VEGFR	Inactive	0.004142	81.60	1.229
BEZ235	915019-65-7	PI3K | mTOR	Inactive	0.00426	104.15	1.282
BI 2536	755038-02-9	PLK	Inactive	0.003834	67.68	2.508
BIBF1120(Vargatef)	928326-83-4	FGFR | VEGFR	Inactive	0.003706	87.94	2.495
BIBW2992(Tovok)	439081-18-2	EGFR | HER2	Inactive	0.004116	66.37	1.713
BIRB 796	285983-48-4	p38 MAPK	Inactive	0.00379	93.51	1.323
BIX 02188	1094614-84-2	MEK	Inactive	0.004689	91.61	1.616
BIX 02189	1094614-85-3	MEK	Inactive	0.00454	85.92	1.435
BMS 777607	1196681-44-3	c-Met	Inactive	0.003899	100.34	3.856
BMS 794833	1174046-72-0	VEGFR | c-Met | FLT-3	1.350289	0.004266	62.14	3.195
BMS-599626	8173837-23-1	EGFR | HER2	Inactive	0.003527	73.23	3.586
Bosutinib(SKI-606)	380843-75-4	ABL	0.5	0.00377	66.01	4.61
BS-181 hydrochloride	1397219-81-6	CDK	1.32514	0.003827	30.11	1.637
CCT129202	942947-93-5	Aurora	Inactive	0.004024	114.75	0.897
Cediranib(AZD2171)	288383-20-0	VEGFR	2.474041	0.004439	79.11	1.401
CHIR-99021	252917-06-9	GSK-3	Inactive	0.004298	111.74	1.227
CI-1033(Canertinib)	267243-28-7	HER2 | EGFR	1.463127	0.002188	29.41	3.074
CI-1040 (PD184352)	212631-79-3	MEK	Inactive	0.004178	89.34	1.664
Colchicine	64-86-8	Tubulin (used as control)	0.83	9.99E-06	57.68	2.091
CP-724714	537705-08-1	HER2	Inactive	0.00426	101.02	2.833
CYC116	693228-63-6	Aurora | VEGFR	3.49107	0.005154	50.61	1.846
Dasatinib	302962-49-8	ABL	Inactive	0.004098	104.94	1.381
Deforolimus(MK-8669)	572924-54-0	mTOR	Inactive	0.00202	70.34	4.036
ENMD-2076	934353-76-1	Aurora | Flt-3 | VEGFR | FGFR	4	0.003805	55.25	1.475
Enzastaurin	170364-57-5	PKC	Inactive	0.003879	97.22	1.369
Erlotinib Hydrochloride	183319-69-9	EGFR	Inactive	0.004652	95.45	5.355
Everolimus(RAD001)	159351-69-6	mTOR	Inactive	0.002087	78.45	2.934
Flavopiridol(Alvocidib)	146426-40-6	CDK	Inactive	0.004977	101.98	3.17
GDC-0879	905281-76-7	RAF	Inactive	0.005981	107.27	2.613
GDC-0941	957054-30-7	PI3K	0.773247	0.003894	70.96	1.355
Gefitinib(Iressa)	184475-35-2	EGFR | Akt	Inactive	0.004475	98.17	1.34
GSK1059615	958852-01-1	PI3K | mTOR	Inactive	0.005999	91.91	1.197
GSK461364	929095-18-1	PLK	0.932748	0.003679	67.68	1.823
Hesperadin	422513-13-1	Aurora	Inactive	0.003871	117.94	1.403
HMN-214	173529-46-9	PLK	Inactive	0.004712	78.79	3.22
IC-87114	371242-69-2	PI3K	Inactive	0.005032	77.10	3.902
Imatinib Mesylate	220127-57-1	c-Kit	Inactive	0.003392	93.35	2.728
Imatinib(STI571)	152459-95-5	VEGFR	Inactive	0.004052	96.58	2.842
Indirubin	479-41-4	GSK-3	Inactive	0.007626	105.11	1.099
JNJ-38877605	943540-75-8	c-Met	Inactive	0.0053	112.36	1.294
JNJ-7706621	443797-96-4	Aurora / CDK	0.985232	0.005072	87.13	1.105
Ki8751	228559-41-9	c-Kit | VEGFR | FGFR	Inactive	0.004261	89.31	2.658
KRN 633	286370-15-8	VEGFR	Inactive	0.004798	95.96	3.172
KU-0063794	938440-64-3	mTOR	Inactive	0.004296	93.50	3.103
KU-55933	587871-26-9	ATM	Inactive	0.005057	46.10	2.876
KU-60019	925701-49-1	ATM	1.329854	0.003652	49.01	1.486

KW 2449	1000669-72-6	FLT-3 | ABL | Aurora	Inactive	0.006017	93.96	4.683
Lapatinib Ditosylate	388082-77-7	EGFR | HER2	Inactive	0.002161	107.82	1.222
LY2228820	862507-23-1	p38 MAPK	Inactive	0.003264	88.96	1.558
LY2784544	1229236-86-5	JAK	Inactive	0.004256	124.76	2.605
LY294002	154447-36-6	PI3K	Inactive	0.006507	104.73	2.668
Masitinib(AB1010)	790299-79-5	c-Kit | FGFR | VEGF	1.658041	0.002381	20.79	2.985
MGCD-265	875337-44-3	c-Met | VEGFR | Tie-2	Inactive	0.003864	105.43	1.658
MK-2206	1032350-13-2	Akt	Inactive	0.004163	103.46	1.895
MLN8237	1028486-01-2	Aurora	Inactive	0.003854	112.75	2.064
Motesanib Diphosphate	857876-30-3	VEGFR | PDGFR | Src	Inactive	0.003512	108.22	4.405
MP-470	850879-09-3	c-Kit | c-Met | FLT-3	Inactive	0.004469	81.09	1.33
Neratinib	698387-09-6	HER2	0.982039	0.000981	27.53	1.256
Nilotinib	641571-10-0	ABL	Inactive	0.003777	88.81	2.476
NVP-ADW742	475488-23-4	IGF-1R	1.830101	0.002036	20.36	1.654
NVP-TAE684	761439-42-3	ALK	Inactive	0.003256	101.89	1.703
ON-01910	1225497-78-8	PLK	0.5	0.004224	63.38	1.907
OSI-930	728033-96-3	c-Kit | VEGFR	Inactive	0.00451	97.12	1.02
Pazopanib Hydrochloride	635702-64-6	VEGFR	Inactive	0.00422	66.52	1.706
PD0325901	391210-10-9	MEK	Inactive	0.004148	100.07	3.427
PD0332991	571190-30-2	CDK	Inactive	0.004469	81.42	0.8376
PD153035 hydrochloride	183322-45-4	EGFR	Inactive	0.005042	93.13	2.898
PD318088	391210-00-7	MEK	Inactive	0.003564	99.32	1.363
PD98059	167869-21-8	MEK	Inactive	0.007483	99.51	0.6507
Pelitinib	257933-82-7	EGFR	Inactive	0.004274	83.19	1.65
PF-04217903	956905-27-4	c-Met	Inactive	0.005371	102.16	2.132
PF-2341066	877399-52-5	c-Met | ALK	2.685256	0.002787	23.22	3.008
PHA-680632	398493-79-3	Aurora	Inactive	0.003987	83.88	1.548
PHA-739358(Danusertib)	827318-97-8	Aurora | ABL	Inactive	0.004214	111.40	4.365
PHA-793887	718630-59-2	CDK	Inactive	0.005533	116.61	3.269
PI-103	371935-74-9	PI3K | mTOR	Inactive	0.005741	57.40	1.049
PIK-293	900185-01-5	PI3K	Inactive	0.005032	82.23	3.32
PIK-75 Hydrochloride	372196-77-5	PI3K	Inactive	0.004092	97.86	1.717
PIK-90	677338-12-4	PI3K	Inactive	0.005692	105.53	2.201
PIK-93	593960-11-3	PI3K	Inactive	0.00513	110.54	1.635
PLX-4720	918505-84-7	RAF	Inactive	0.004833	114.53	1.222
Quercetin(Sophoretin)	117-39-5	PI3K | PKC	Inactive	0.006617	105.81	1.439
R406	841290-81-1	Syk	Inactive	0.003182	107.39	1.344
R406(free base)	841290-80-0	Syk	Inactive	0.004251	107.15	1.487
RAF265	927880-90-8	RAF| VEGFR	Inactive	0.003858	93.09	1.718
Rapamycin(Sirolimus)	53123-88-9	mTOR	Inactive	0.002188	109.89	2.509
Roscovitine(CYC202)	186692-46-6	CDK	Inactive	0.005643	106.75	1.782
SB 202190	152121-30-7	p38 MAPK	Inactive	0.006036	97.11	1.683
SB 203580	152121-47-6	p38 MAPK	1.140681	0.005299	80.54	1.644
SB 216763	280744-09-4	GSK-3	Inactive	0.005388	107.30	0.8033
SB 431542	301836-41-9	ALK	Inactive	0.005203	67.24	3.57
SB 525334	356559-20-1	ALK	Inactive	0.005824	89.56	4.03
SGX-523	1022150-57-7	c-Met	Inactive	0.005565	106.20	1.444
SNS-032(BMS-387032)	345627-80-7	CDK	Inactive	0.005256	103.27	1.636
SNS-314 Mesylate	1057249-41-8	Aurora	1.743522	0.002217	26.41	2.724
Sorafenib Tosylate	475207-59-1	VEGFR | RAF | MEK	2.489475	0.002209	30.23	2.589
SP600125	129-56-6	JNK	Inactive	0.009082	108.28	4.468
SU11274(PKI-SU11274)	658084-23-2	c-Met	0.59355	0.003521	45.65	0.9738
Sunitinib Malate	341031-54-7	FLT-3 | VEGFR | Kit	1.858937	0.003755	74.73	1.143
Tandutinib (MLN518)	387867-13-2	FLT-3 | c-KIT	Inactive	0.003554	72.58	1.502
Temsirolimus	162635-04-3	mTOR	Inactive	0.001941	77.26	1.683
TG100-115	677297-51-7	PI3K	Inactive	0.005775	97.79	0.89
TGX-221	663619-89-4	PI3K	Inactive	0.005488	96.74	3.572
TSU-68	252916-29-3	VEGFR | FGFR	Inactive	0.006444	100.62	3.294
U0126-EtOH	1173097-76-1	MEK	Inactive	0.004689	106.00	1.296
Vandetanib	443913-73-3	VEGFR | EGFR	1.393366	0.004207	61.62	2.716
Vatalanib	212141-51-0	VEGFR | c-Kit | FLT-3	Inactive	0.004765	85.99	2.543
Vinorelbine(Navelbine)	71486-22-1	p38 MAPK	1.117829	8.11E-07	42.42	4.42
VX-680	639089-54-6	Aurora	Inactive	0.004305	76.51	0.9318
VX-702	479543-46-9	p38 MAPK	Inactive	0.004947	91.18	3.594
VX-745	209410-46-8	p38 MAPK	Inactive	0.004584	89.65	7.681
WYE-354	1062169-56-5	mTOR	Inactive	0.004036	79.09	1.378
WZ3146	1214265-56-1	EGFR	Inactive	0.004302	90.65	0.8991
WZ4002	1213269-23-8	EGFR	Inactive	0.004041	104.65	1.124
WZ8040	1214265-57-2	EGFR	1.141569	0.004158	55.28	1.323

XL147	956958-53-5	PI3K	Inactive	0.004459	102.91	1.96
XL184	849217-68-1	c-Met | FLT-3 | VEGFR | c-KIT	Inactive	0.003988	94.78	1.664
XL765	1123889-87-1	PI3K	Inactive	0.003335	110.36	0.9356
XL880(GSK1363089)	849217-64-7	c-Met | VEGFR	1.658425	0.00265	33.19	4.216
ZM-447439	331771-20-1	Aurora	Inactive	0.003894	90.86	1.728
ZSTK474	475110-96-4	PI3K	Inactive	0.004791	98.86	0.9774

Supplementary Table II

Compound ID	CAS number	Target	nHill	qAC50	Residual activity (Median)	Standard error
ABT-869(Linifanib)	796967-16-3	VEGFR	Inactive	0.005328	111.40	1.942
AC-220	950769-58-1	FLT-3	1.436358	0.000172	85.88	1.661
AEE788	497839-62-0	EGFR | HER1/2 | VEGFR | Flt-1	0.5	0.004539	64.52	5.119
AG-490	133550-30-8	EGFR | JAK	Inactive	NA	62.46	2.87
AP24534	943319-70-8	VEGFR | FGFR | FLT-3	Inactive	NA	51.61	5.275
AS-605240	648450-29-7	PI3K	Inactive	0.007774	116.43	3.648
AS703026	1236699-92-5	MEK	Inactive	0.004638	105.53	3.084
AT7519	844442-38-2	CDK	Inactive	0.005232	104.77	1.734
AT7867	857531-00-1	Akt	0.606294	0.00592	70.96	4.514
AT9283	896466-04-9	Aurora | JAK | ABL	Inactive	0.005243	49.39	5.075
Aurora A Inhibitor I	1158838-45-9	Aurora	Inactive	0.003401	95.01	4.459
AV-951(Tivozanib)	475108-18-0	VEGFR	Inactive	0.004397	69.21	5.143
Axitinib	319460-85-0	VEGFR	0.5	0.005175	60.78	1.488
AZD0530(Saracatinib)	379231-04-6	ABL	0.637742	0.00369	51.85	2.335
AZD1152-HQPA(Barasertib)	722544-51-6	Aurora	Inactive	0.00394	105.80	2.339
AZD1480	935666-88-9	JAK	2.48508	0.005735	142.14	2.618
AZD6244(Selumetinib)	606143-52-6	MEK	Inactive	0.00437	96.22	2.489
AZD6482	1173900-33-8	PI3K	Inactive	0.004897	131.95	1.131
AZD7762	860352-01-8	CHK	Inactive	0.005518	127.72	1.749
AZD8055	1009298-09-2	mTOR	Inactive	0.004296	102.97	1.692
AZD8330	869357-68-6	MEK	Inactive	0.004336	101.27	3.425
BAY 73-4506(Regorafenib)	755037-03-7	c-KIT | VEGFR	0.5	0.003432	62.47	3.282
BEZ235	915019-65-7	PI3K | mTOR	Inactive	0.00426	128.01	1.958
BI 2536	755038-02-9	PLK	0.5	0.001663	61.08	4.656
BIBF1120(Vargatef)	928326-83-4	FGFR | VEGFR	2.337782	2.24E-05	53.12	2.551
BIBW2992(Tovok)	439081-18-2	EGFR | HER2	0.5	0.003091	50.84	4.105
BIRB 796	285983-48-4	p38 MAPK	Inactive	0.00379	94.18	1.4
BIX 02188	1094614-84-2	MEK	0.5	0.004689	69.52	1.975
BIX 02189	1094614-85-3	MEK	1.406958	0.00454	68.90	1.77
BMS 777607	1196681-44-3	c-Met	Inactive	NA	81.06	5.612
BMS 794833	1174046-72-0	VEGFR | c-Met | FLT-3	0.67305	0.004266	69.82	5.162
BMS-599626	8173837-23-1	EGFR | HER2	3.623089	0.003527	96.94	4.239
Bosutinib(SKI-606)	380843-75-4	ABL	0.5	0.002486	50.52	5.168
BS-181 hydrochloride	1397219-81-6	CDK	Inactive	NA	28.92	2.644
CCT129202	942947-93-5	Aurora	Inactive	0.004024	99.49	1.772
Cediranib(AZD2171)	288383-20-0	VEGFR	0.695237	0.002018	48.94	2.098
CHIR-99021	252917-06-9	GSK-3	Inactive	0.004298	101.87	2.837
CI-1033(Canertinib)	267243-28-7	HER2 | EGFR	0.797796	0.001326	38.08	5.456
CI-1040 (PD184352)	212631-79-3	MEK	4	6.62E-06	47.43	1.867
Colchicine	64-86-8	Tubulin (used as control)	0.8	9.74E-06	58.11	1.419
CP-724714	537705-08-1	HER2	Inactive	0.00426	104.76	4.142
CYC116	693228-63-6	Aurora | VEGFR	2.599212	0.002925	20.33	4.053
Dasatinib	302962-49-8	ABL	Inactive	0.004098	91.41	2.37
Deforolimus(MK-8669)	572924-54-0	mTOR	Inactive	NA	56.18	3.082
ENMD-2076	934353-76-1	Aurora | Flt-3 | VEGFR | FGFR	1.654872	0.002733	38.09	2.029
Enzastaurin	170364-57-5	PKC	Inactive	0.003879	99.63	1.711
Erlotinib Hydrochloride	183319-69-9	EGFR	4	4.07E-07	70.95	6.794
Everolimus(RAD001)	159351-69-6	mTOR	Inactive	NA	73.76	2.527
Flavopiridol(Alvocidib)	146426-40-6	CDK	Inactive	NA	65.94	4.419
GDC-0879	905281-76-7	RAF	Inactive	0.005981	113.93	4.043
GDC-0941	957054-30-7	PI3K	2.627782	0.002188	19.21	1.756
Gefitinib(Iressa)	184475-35-2	EGFR | Akt	Inactive	0.004475	124.05	2.182
GSK1059615	958852-01-1	PI3K | mTOR	Inactive	0.005999	89.96	2.697
GSK461364	929095-18-1	PLK	0.580974	0.000844	39.78	3.107
Hesperadin	422513-13-1	Aurora	1.315694	5.01E-05	149.34	1.415
HMN-214	173529-46-9	PLK	0.5	0.004712	76.33	5.656
IC-87114	371242-69-2	PI3K	Inactive	NA	55.96	3.487
Imatinib Mesylate	220127-57-1	c-Kit	0.5	0.003392	92.22	3.616
Imatinib(STI571)	152459-95-5	VEGFR	Inactive	0.004052	102.13	3.291
Indirubin	479-41-4	GSK-3	Inactive	0.007626	119.93	2.1
JNJ-38877605	943540-75-8	c-Met	Inactive	0.0053	103.29	1.764
JNJ-7706621	443797-96-4	Aurora / CDK	Inactive	0.005072	92.60	2.659
Ki8751	228559-41-9	c-Kit | VEGFR | FGFR	Inactive	NA	65.93	3.54
KRN 633	286370-15-8	VEGFR	4	0.00096	63.98	2.755
KU-0063794	938440-64-3	mTOR	Inactive	0.004296	96.81	3.788
KU-55933	587871-26-9	ATM	Inactive	NA	30.02	3.853
KU-60019	925701-49-1	ATM	4	0.003652	44.93	2.368

KW 2449	1000669-72-6	FLT-3 | ABL | Aurora	0.5	0.006017	89.39	5.942
Lapatinib Ditosylate	388082-77-7	EGFR | HER2	Inactive	0.002161	105.91	1.289
LY2228820	862507-23-1	p38 MAPK	Inactive	0.003264	88.18	1.962
LY2784544	1229236-86-5	JAK	Inactive	0.004256	124.83	2.689
LY294002	154447-36-6	PI3K	3.774832	0.006507	110.19	3.435
Masitinib(AB1010)	790299-79-5	c-Kit | FGFR | VEGF	0.5	0.002422	28.02	6.116
MGCD-265	875337-44-3	c-Met | VEGFR | Tie-2	0.5	0.003512	70.10	2.341
MK-2206	1032350-13-2	Akt	Inactive	0.004163	80.04	4.248
MLN8237	1028486-01-2	Aurora	Inactive	0.003854	93.55	2.406
Motesanib Diphosphate	857876-30-3	VEGFR | PDGFR | Src	4	0.003512	100.69	4.224
MP-470	850879-09-3	c-Kit | c-Met | FLT-3	Inactive	0.004469	78.92	2.749
Neratinib	698387-09-6	HER2	4	0.000432	30.20	2.01
Nilotinib	641571-10-0	ABL	Inactive	0.003777	97.63	3.206
NVP-ADW742	475488-23-4	IGF-1R	1.690275	0.000264	33.84	3.012
NVP-TAE684	761439-42-3	ALK	Inactive	0.003256	106.20	2.016
ON-01910	1225497-78-8	PLK	1.191079	5.85E-05	69.64	2.724
OSI-930	728033-96-3	c-Kit | VEGFR	Inactive	0.00451	85.38	2.42
Pazopanib Hydrochloride	635702-64-6	VEGFR	1.323082	0.00422	58.02	1.478
PD0325901	391210-10-9	MEK	Inactive	0.004148	99.74	4.176
PD0332991	571190-30-2	CDK	4	9.03E-07	36.16	1.822
PD153035 hydrochloride	183322-45-4	EGFR	0.5	0.005042	77.89	2.34
PD318088	391210-00-7	MEK	Inactive	0.003564	98.15	1.448
PD98059	167869-21-8	MEK	Inactive	0.007483	112.56	1.394
Pelitinib	257933-82-7	EGFR	1.28075	0.000135	57.97	2.581
PF-04217903	956905-27-4	c-Met	Inactive	0.005371	104.95	4.045
PF-2341066	877399-52-5	c-Met | ALK	1.093137	0.001765	30.19	3.104
PHA-680632	398493-79-3	Aurora	0.627183	0.003987	63.42	2.356
PHA-739358(Danusertib)	827318-97-8	Aurora | ABL	4	0.004214	139.90	3.855
PHA-793887	718630-59-2	CDK	Inactive	0.005533	129.45	4.285
PI-103	371935-74-9	PI3K | mTOR	Inactive	NA	45.49	2.69
PIK-293	900185-01-5	PI3K	Inactive	NA	71.33	3.889
PIK-75 Hydrochloride	372196-77-5	PI3K	Inactive	0.004092	101.69	4.919
PIK-90	677338-12-4	PI3K	Inactive	0.005692	93.77	3.314
PIK-93	593960-11-3	PI3K	0.5	0.001026	80.99	2.022
PLX-4720	918505-84-7	RAF	Inactive	0.004833	115.72	2.523
Quercetin(Sophoretin)	117-39-5	PI3K | PKC	Inactive	0.006617	92.57	1.533
R406	841290-81-1	Syk	Inactive	0.003182	99.47	2.37
R406(free base)	841290-80-0	Syk	Inactive	0.004251	102.03	1.87
RAF265	927880-90-8	RAF| VEGFR	Inactive	0.003858	91.53	2.358
Rapamycin(Sirolimus)	53123-88-9	mTOR	Inactive	0.002188	92.67	4.319
Roscovitine(CYC202)	186692-46-6	CDK	Inactive	0.005643	98.59	4.712
SB 202190	152121-30-7	p38 MAPK	Inactive	0.006036	111.95	2.016
SB 203580	152121-47-6	p38 MAPK	2.671028	0.00496	51.74	2.328
SB 216763	280744-09-4	GSK-3	Inactive	0.005388	115.07	1.812
SB 431542	301836-41-9	ALK	Inactive	0.005203	68.30	6.089
SB 525334	356559-20-1	ALK	Inactive	NA	67.80	5
SGX-523	1022150-57-7	c-Met	Inactive	0.005565	105.20	0.8619
SNS-032(BMS-387032)	345627-80-7	CDK	Inactive	0.005256	91.11	3.691
SNS-314 Mesylate	1057249-41-8	Aurora	0.709306	0.001203	28.64	3.885
Sorafenib Tosylate	475207-59-1	VEGFR | RAF | MEK	1.661538	0.001545	26.49	3.673
SP600125	129-56-6	JNK	Inactive	0.009082	113.79	5.058
SU11274(PKI-SU11274)	658084-23-2	c-Met	0.5	0.000427	22.71	1.466
Sunitinib Malate	341031-54-7	FLT-3 | VEGFR | Kit	0.819447	0.003755	57.09	1.194
Tandutinib (MLN518)	387867-13-2	FLT-3 | c-KIT	Inactive	NA	49.98	2.681
Temsirolimus	162635-04-3	mTOR	4	0.001941	104.51	2.349
TG100-115	677297-51-7	PI3K	Inactive	0.005775	106.47	1.064
TGX-221	663619-89-4	PI3K	Inactive	0.005488	109.95	3.552
TSU-68	252916-29-3	VEGFR | FGFR	Inactive	0.006444	97.45	5.416
U0126-EtOH	1173097-76-1	MEK	Inactive	0.004689	101.67	1.771
Vandetanib	443913-73-3	VEGFR | EGFR	0.922011	0.001273	26.65	4.188
Vatalanib	212141-51-0	VEGFR | c-Kit | FLT-3	Inactive	NA	50.31	2.3
Vinorelbine(Navelbine)	71486-22-1	p38 MAPK	0.5	2.52E-06	41.79	2.146
VX-680	639089-54-6	Aurora	0.5	0.004305	62.61	2.246
VX-702	479543-46-9	p38 MAPK	Inactive	0.004947	96.01	4.057
VX-745	209410-46-8	p38 MAPK	Inactive	0.004584	85.93	4.995
WYE-354	1062169-56-5	mTOR	0.5	0.004036	67.35	2.602
WZ3146	1214265-56-1	EGFR	Inactive	0.004302	80.62	2.649
WZ4002	1213269-23-8	EGFR	Inactive	0.004041	93.25	2.071
WZ8040	1214265-57-2	EGFR	1.58971	0.003539	46.43	1.866

XL147	956958-53-5	PI3K	Inactive	0.004459	115.14	1.518
XL184	849217-68-1	c-Met | FLT-3 | VEGFR | c-KIT	Inactive	0.003988	102.47	2.262
XL765	1123889-87-1	PI3K	Inactive	0.003335	113.85	2.006
XL880(GSK1363089)	849217-64-7	c-Met | VEGFR	0.556082	0.00238	31.28	3.487
ZM-447439	331771-20-1	Aurora	0.976484	1.55E-05	81.73	3.426
ZSTK474	475110-96-4	PI3K	Inactive	0.004791	106.50	2.439

SUPPLEMENTAL MATERIAL
Material and Methods

Cell culture

Human aortic endothelial cells (HAECs) from Cell Applications Inc (304-05a), were cultured in endothelial cell basal medium (LONZA Clonetics CC-3156 or ATCC PCS-100-030) with 5% fetal bovine serum (GIBCO), 100U/mL of penicillin and 100µg/mL streptomycin (Sigma-Aldrich), supplemented with singleQuots (LONZA Clonetics CC-4176 or ATCC PCS-100-041, containing hFGF, hVEGF, hIGF-1, hEGF, hydrocortisone, ascorbic acid, heparin) hereafter referred to as medium A or singleQuots without VEGF, hereafter referred to as medium B at 37ºC in a humidified 5% CO_2, 95% air incubator. According to the product description by ATCC, medium A contains 5 ng/ml VEGF-A. Lonza does not provide any public information on the VEGF-A content of its medium A. For some experiments (if indicated) we supplemented the VEGF-free medium B with 25 ng/ml VEGF-A (Sigma, V7259)

Lipoprotein Isolation and labeling

LDL (1.019<d<1.063 g/mL) and HDL (1.063<d<1.21 g/mL) were isolated from fresh human normolipidemic plasma of blood donors by sequential ultracentrifugation as described previously [1, 2]. LDL and HDL were fluorescently labeled with Atto-488 (Atto-Tec, AD 488-35) and Atto-594-NHS-ester dyes, respectively (Atto-Tec, AD 594-35). The reaction was performed at a pH 8.0 adjusted by adding 1M $NaHCO_3$ to obtain a final concentration of 0.1M in dark at room temperature for 1hour. The labeled lipoproteins were separated from free dye by gel filtration chromatography using PD-10 desalting columns (GE healthcare, 170851-01). LDL and HDL were radioiodinated with $Na^{125}I$ by the McFarlane monochloride procedure modified for lipoproteins [2, 3]. Specific activities between 300-900 cpm/ ng of protein were obtained.

Kinase inhibitor screen

HAECs were seeded in 384 well plates (BD falcon, 353962) using a washer dispenser (Biotek, EL406), at a density of 1000 cells per well in medium A and cultured for 72 hours at 37ºC in a humidified 5% CO_2, 95% air incubator. Following culture, cells were treated with a 141 drugs encompassing kinase inhibitor library (Selleckchem, L1200). For each drug, seven different concentrations were used at a dilution range of 128, 640, 3200, 16000, 80000, 400000, 2000000. After 1 hour of drug treatment, cells were incubated with fluorescent labeled Atto594-HDL and LDL [RFP (Red fluorescent protein) channel] for another hour. The cells were later washed with PBS using 384-well head manifold (Biotek, EL406), fixed with 2% paraformaldehyde and nuclei were stained with Hoechst- 33258 (Sigma, 861405). Nine images per well were acquired with 20x objective using widefield microscope (Molecular devices). The microscope generated images were processed by Cell profiler to segment nuclei and RFP foci intensity (HDL and LDL vesicles) per cell. Fitting of RFP foci per cell values as a function of drug-concentration was done in Genedata Screener (Genedata, Basel, Switzerland). The formula used to fit the dose-response data was a logistic function of the Hill Model type.

$$Y(X) = S_\infty + \frac{S_0 - S_\infty}{1 + (X/\ IC_{50})^{nHill}}$$

where X is the drug concentration, Y is the activity, S_0 is fitted activity level at zero concentration (zero activity), S_∞ is fitted activity level at infinite concentration (infinite activity),

nHill is the Hill coefficient for the curve which is the measure of the slope at IC_{50}, IC_{50} is the concentration at which the uptake of fluorescent HDL or LDL was inhibited by 50%. The fit parameters were constrained so that $0.5 \leq nHill \leq 4$, $S_0 = 0$, $S_\infty = -100$. Prior to applying the Fisher exact test analysis, the drugs were classified as active based on the possibility to fit Hill model, and the rest of the drugs were assigned as inactive. The only arbitrary feature of this procedure is the choice to fit the logistic model only when the fluorescent signal drop was more than 50%. The reproducibility of the dose-response curves for foci per cell was assessed by the performance of two independent duplicate experiments.

Small Interfering RNA Transfection

Endothelial cells were reverse transfected with small interfering RNA (Ambion silencer select, Life technologies) targeted to VEGFR1 (s5287, s5288) or VEGFR2 (s7822, s7824) or VEGFR3 (s5294, s5295) or AKT (s659, s660) or MAPK14 (p38 MAPK) (s3585, s3586) or MAP2K1 & MAPK2K2 (MEK1/2) (s11167, s11170) or SR-BI (s2648, s2649, s2650) or non-silencing control (4390843) at a final concentration of 5nmol/L using Lipofectamine RNA iMAX transfection reagent (Invitrogen, 13778150) in an antibiotic-free medium A or B as indicated. All experiments were performed 72 hours post-transfection and efficiency of transfection was confirmed with at least two siRNAs against each gene using quantitative RT-PCR and western blotting.

Quantitative real time PCR

Total RNA was isolated using TRI reagent (Sigma T9424) according to the manufacturer's instruction. Genomic DNA was removed by digestion using DNase (Roche) and RNase inhibitor (Ribolock, Thermo Scientific). Reverse transcription was performed using M-MLVRT (Invitrogen, 200U/µL) following the standard protocol as described by the manufacturer. Quantitative PCR was done with Lightcycler FastStart DNA Master SYBR Green I (Roche) using gene specific primers as followed:

VEGFR1 (For: CTG AAG GAA GGG AGC TCG TC; Rev: GGC GTG GTG TGC TTA TTT GG),
VEGFR2 (For: CGG TCA ACA AAG TCG GGA GA; Rev: CAG TGC ACC ACA AAG ACA CG),
VEGFR3 (For: TCC TAC GTG TTC GTG AGA GAC; Rev: CAC CAG GAA GGG GTT GGA AA),
SR-BI (For: CTG TGG GTG AGA TCA TGT GG; Rev: GCC AGA AGT CAA CCT TGC TC), normalized to GAPDH (For: CCC ATG TTC GTC ATG GGT GT; Rev: TGG TCA TGA GTC CTT CCA CGA TA).

Wide-field Fluorescence Microscopy for coverslips

Endothelial cells were cultured in medium A or medium B as monolayers on coverslips. After 72hours, cells were subjected to treatment as indicated, followed by incubation with 50µg/mL of Atto594 labeled HDL or Atto488 labeled LDL for 1hour at 37 ºC as previously described [4]. Cells were then washed, fixed with 2% paraformaldehyde and images were acquired on a Zeiss Axiovert 200M.

MTT proliferation assay

Endothelial cells were cultured in medium A or medium B at a density of 10^5 cells per well in a 24 well plate. After 72 hours of culture, the supernatant was removed and cells were washed twice with PBS. The cells were then incubated with 30µL of MTT solution (5mg/ml in PBS,Sigma, M5655) diluted in 270µL of DMEM for 1 hour. The resultant formazan salts were

extracted with dimethyl sulfoxide (DMSO) and absorbance intensity was read at 550nm and reference wavelength at 650nm (DMSO). The rate of cell proliferation is calculated relative to the cells cultured in medium A.

Lipoprotein Binding, Cell association and Transport

The methods for the quantification of binding, association and transport of radiolabeled HDL and LDL by endothelial cells have been previously described [2, 5, 6]. All assays were performed in DMEM (Sigma) containing 25mmol/L HEPES and 0.2% BSA instead of serum. Where indicated, cells were pretreated for 30mins at 37 ºC with PI3K inhibitor wortmannin (Sigma, 200nmol/L) or Akt inhibitor MK2206 (Selleckchem, 1µmol/L) or Raf/MEK/ERK inhibitor U0126 (Abcam, 10µmol/L) or p38MAPK inhibitor PD169316 (Calbiochem, 100nmol/L), followed by pre-treatment with VEGF-A_{165} (Sigma, 25ng/ml) for 1hr at 37 ºC. Following treatments, the cells were incubated with 10µg/mL of ^{125}I-HDL/ LDL without (total) or with a 40 times excess of non-labeled HDL/ LDL (unspecific) for 1hr at 4 ºC for cellular binding and at 37ºC for association and transport experiments. Specific cellular binding/ association/ transport was calculated by subtracting the values obtained in the presence of excess unlabeled HDL/ LDL (unspecific) from those obtained in the absence of unlabeled HDL/ LDL (total).

Western Blotting

Endothelial cells were lysed in RIPA buffer (10mmol/L Tris pH 7.4, 150mmol/L NaCl, 1% NP-40, 1% sodium deoxycholate, 0.1% SDS, complete EDTA (Roche)) with protease and phosphotase inhibitors. Equal amounts of protein were separated on SDS-PAGE and trans-blotted onto PVDF membrane (GE Healthcare). Membranes were blocked in appropriate blocking buffer recommended for the antibody (TBS-T supplemented with 5% milk or BSA) and incubated either for 1hour or overnight on shaker at 4 ºC with primary antibodies at a dilution of 1:1000 in the same blocking buffer. Membranes were incubated for 1hour with HRP-conjugated secondary antibody (Dako) in blocking buffer at a dilution of 1:2500. Membranes were further incubated with chemiluminescence substrate for 1min (Pierce ECL plus, Thermo scientific) and imaged using Fusion Fx (Vilber). As indicated Beta-Actin, GAPDH or TATA binding protein was used as loading control with primary antibody at 1:5000 and secondary antibody at 1:10000 dilutions. The silencing efficiencies of VEGFR1 (2893, CST), VEGFR2 (9686, CST) and VEGFR3 (ab27278, Abcam) were evaluated and compared to Beta-Actin (ab8226, Abcam). The expression of SR-BI (NB400-131, Novus) was evaluated and compared to the expression of GAPDH (ab9484, Abcam). The silencing efficiencies of Akt (9272, CST), p38 MAPK (9212, CST) and MEK1/2 (8727, CST) were compared to TATA binding protein (TBP, ab51841, Abcam). The Phospho-expressions of VEGFR2 (3817, CST), Akt S473 (9271, CST), p38 MAPK Thr180/Tyr182 (9211, CST), p44/42 MAPK Thr202/Tyr204 & Thr185/Tyr187 (9106, CST) were compared to the total expression of VEGFR2 (9698, CST), Akt (9272, CST), p38 MAPK (9212, CST) and p44/42 MAPK (4695, CST) respectively.

Cell surface expression analysis

Biotinylation of intact cells was performed using 20mg/mL EZ-Link sulfo-NHS-S-S-Biotin (Thermo Scientific) in the cold for 1 hour with mild shaking and quenched with ice-cold Tris pH 7.4. Cells were lysed in RIPA buffer (total cell lysate) and 200-500µg of lysates were incubated with 20µL of BSA- blocked streptavidin beads suspension (GE Healthcare) for 16hours at 4 ºC and pelleted by centrifugation; the pellet represents surface proteins. Proteins were dissociated from the pellet by boiling with SDS loading buffer and analyzed by SDS-PAGE and

immunoblotting with SR-BI antibody (NB400-131, Novus) and LDL receptor (LDLR, ab30532, Abcam), ABCG1 (NB400-132, Novus). TATA binding protein (TBP, ab51841, Abcam) and endothelial lipase (EL,NB400-118, Novus) were used as intracellular and plasma membrane controls.

Statistical Analysis

Probability of finding active and inactive drugs for a given target compared to non-targeting drugs was performed using Fisher exact test analysis. The drugs were pre-classified as active based on their ability to fit the Hill logistic model only when the RFP foci signal dropped more than 50%. The data sets for all validation experiments were analyzed using the GraphPad Prism 5 software. Comparison between groups in follow up biochemical validation experiments was performed using Kruskal-Wallis one-way ANOVA followed by Dunn's post test. The data was obtained from at least three independent experiments, performed in triplicates or quadruplets. Values are expressed as mean±SEM. $P<0.05$ was regarded as significant.

References

1. Havel RJ, Eder HA, Bragdon JH. The distribution and chemical composition of ultracentrifugally separated lipoproteins in human serum. *J Clin Invest.* 1955;**34**:1345-1353.
2. Rohrer L, Cavelier C, Fuchs S, Schluter MA, Volker W, von Eckardstein A. Binding, internalization and transport of apolipoprotein A-I by vascular endothelial cells. *Biochim Biophys Acta.* 2006;**1761**:186-194.
3. Freeman M, Ekkel Y, Rohrer L, Penman M, Freedman NJ, Chisolm GM, et al. Expression of type I and type II bovine scavenger receptors in Chinese hamster ovary cells: lipid droplet accumulation and nonreciprocal cross competition by acetylated and oxidized low density lipoprotein. *Proc Natl Acad Sci U S A.* 1991;**88**:4931-4935.
4. Perisa D, Rohrer L, Kaech A, von Eckardstein A. Itinerary of high density lipoproteins in endothelial cells. *Biochim Biophys Acta.* 2016;**1861**:98-107.
5. Cavelier C, Rohrer L, von Eckardstein A. ATP-Binding cassette transporter A1 modulates apolipoprotein A-I transcytosis through aortic endothelial cells. *Circ Res.* 2006;**99**:1060-1066.
6. Rohrer L, Ohnsorg PM, Lehner M, Landolt F, Rinninger F, von Eckardstein A. High-density lipoprotein transport through aortic endothelial cells involves scavenger receptor BI and ATP-binding cassette transporter G1. *Circ Res.* 2009;**104**:1142-1150.